

Investigation of Occupational Dose to Interventional Radiologists

by

Millicent P. Tysinger

Graduate Program in Medical Physics
Duke University

Date: _____

Approved:

Chu Wang, Supervisor

Terry Yoshizumi

Robert Reiman

Steve Mann

Rathnayaka Gunasingha

Dean Darnell

Thesis submitted in partial fulfillment of
the requirements for the degree of Master of Science
in the Graduate Program in Medical Physics
in the Graduate School of Duke University

2023

ABSTRACT

Investigation of Occupational Dose to Interventional Radiologists

by

Millicent P. Tysinger

Graduate Program in Medical Physics
Duke University

Date: _____

Approved:

Chu Wang, Supervisor

Terry Yoshizumi

Robert Reiman

Steve Mann

Rathnayaka Gunasingha

Dean Darnell

An abstract of a thesis submitted in partial
fulfillment of the requirements for the degree
of Master of Science in the Graduate Program in
Medical Physics in the Graduate School of
Duke University

2023

Copyright by
Millicent P. Tysinger
2023

Abstract

Project 1: Measuring the Effects on Operator Dose of Changing Clinical Settings

Purpose: This study was initiated as part of a multi-faceted investigation of occupational dose to Interventional Radiologists consequential to their role as operators of fluoroscopy equipment. This project aims to qualitatively evaluate general dose reduction techniques, including clinical protocol settings on different interventional fluoroscopes to determine the specific impact on operator dose at Duke University Hospital.

Materials and Methods: For each unit, analogous baseline settings were selected with a general abdominal protocol. The patient table was set to a source-to-object distance (SOD) of 62.2 cm (24.5 in) and a patient phantom was placed in the beam as a scatter medium similar to a typical patient abdomen. An anthropomorphic “operator” phantom was draped with a lead apron and positioned to one side of the patient table with an ion chamber placed at collar level. The ion chamber was placed such that the center of the active volume was 38.1 cm (15 in) lateral to and 63.5 cm (25 in) inferior from the center of the flat-paneled detector. A series of scans was taken on each unit, with each one having a selected variable changed, and the exposure readings from the ion chamber were recorded for comparison.

Results: The effects on operator exposure rate of personnel height, contour shield use, cine mode, magnification, low dose mode, and source-to-image distance (SID) were

analyzed. Operator height was found to have a larger effect on exposure rate reduction with distance than anticipated. Use of the contour shield reduced the operator exposure rate by over 90% on each unit. Use of cine mode drastically increased the exposure rate to the operator, while magnification, low dose mode, and decreasing SID all resulted in lower exposure rates.

Conclusions: Operators can utilize these results to contextualize the effects of their own dose reduction techniques. Knowledge and familiarity of the techniques which offer the best exposure rate reduction can guide radiation protection practices among staff and help to optimize occupational doses.

Project 2: Developing a Conceptual Framework for Analyzing the Radiation Dose Structured Report

Purpose: When investigating occupational doses to Interventional Radiologists, it is important to be able to accurately compare metrics related to doses from historical procedures. The Radiation Dose Structured Report (RDSR) provides characteristic data from historical procedures. With an appropriate framework for analyzing RDSR data, performance metrics between operators or units can be compared, and identified trends can be used to develop dose reduction techniques specific to the organization.

Materials and Methods: RDSR data from five interventional fluoroscopy systems (K1 – K5) was extracted for a three-year period from July 2019 through August 2022, and multiple metrics of comparison were selected for analysis. To determine differences in machine output, air kerma rates of similar procedures were compared, as well as the

overall machine utilization for each year. Differences in operator-selectable variable were compared through air kerma rate per procedure, fluoroscopy time per procedure (limited to central line procedures), and operator caseload makeup.

Results: Machine comparison of air kerma rates showed a consistently higher median and variability on the Philips Allura systems compared to the other three units. The Philips AlluraClarity unit in suite K2 was noticeably under-utilized by Interventional Radiology staff due to it being the primary fluoroscope used by Neurosurgery staff who were outside the scope of this investigation. Operator air kerma rates were compared from August 2021 through August 2022 and largely showed similar median values and variability. Fluoroscopy time per procedure fit to lognormal distributions and compared through their distribution parameter μ showed a median value which dipped during the second year for most operators. One operator also had a consistently higher median time per procedure for all three years.

Conclusions: The analysis described by this framework provides a means of utilizing RDSR data to compare performance of interventional procedures. Continual local analysis of these metrics can be used to guide operator training to ensure that occupational doses are optimized to be as low as reasonably achievable. This is an initial approach that can be expanded through investigation and further characterization of procedure data included in the RDSR.

Contents

Abstract	iv
List of Tables	x
List of Figures	xii
Acknowledgements	xv
Chapter 1. Introduction.....	1
1.1 Interventional Radiology.....	1
1.2 Fluoroscopy Guided IR.....	1
1.2.1 X-ray production	2
1.2.2 X-ray tubes.....	2
1.2.3 X-ray interactions with matter.....	3
1.2.4 Fluoroscopy Systems and Key Characteristics.....	5
1.3 Occupational exposure limits and radiation protection in IR.....	8
1.4 IR at Duke University Hospital	11
1.5 Challenges in evaluating radiation dose to operators.....	12
1.6 Goals.....	12
Chapter 2. Measuring the Effects of Changing Clinical Settings on Operator Dose	14
2.1 Introduction.....	14
2.2 Materials and Methods	15
2.2.1 Phantom Setup and Shielding	15
2.2.2 Clinical Parameters and Variables	17
2.3 Results	20

2.3.1 Provider Height	20
2.3.2 Contour shield use	21
2.3.3 Cine Mode	22
2.3.4 Magnification	23
2.3.5 Low Dose Mode.....	24
2.3.6 SID	25
2.4 Discussion.....	25
2.4.1 Provider Height	25
2.4.2 Contour Shield Use	27
2.4.3 Cine Mode	28
2.4.4 Magnification	29
2.4.5 Low Dose Mode.....	30
2.4.6 SID	32
Chapter 3. Conceptual Framework for Analyzing the Radiation Dose Structured Report (RDSR)	34
3.1 Machine-Specific Differences.....	34
3.1.1 Materials and Methods.....	36
3.1.1.1 Machine Performance.....	36
3.1.1.2 Machine Utilization	37
3.1.2 Results	37
3.1.2.1 Machine Performance.....	37
3.1.2.2 Machine Utilization	42
3.1.3 Discussion.....	44

3.1.3.1 Machine Performance.....	44
3.1.3.2 Machine Utilization	45
3.2 Operator-Specific Differences.....	46
3.2.1 Materials and Methods.....	47
3.2.1.1 AKR Comparison.....	47
3.2.1.2 Fluoroscopy Time Comparison.....	47
3.2.1.3 Caseload Breakdown.....	48
3.2.2 Results	48
3.2.2.1 AKR Comparison.....	48
3.2.2.2 Fluoroscopy Time Comparison.....	68
3.2.2.3 Caseload Breakdown.....	74
3.2.3 Discussion.....	76
3.2.3.1 AKR Comparison.....	76
3.2.3.2 Fluoroscopy Time Comparison.....	77
3.2.3.3 Caseload Breakdown.....	79
Chapter 4: Conclusion	81
References	85

List of Tables

Table 1.1: Radiation exposure annual limits for occupational workers	9
Table 1.2: DUH IR system information.....	11
Table 2.1: Clinical settings for K1 and K2 data collection	18
Table 2.2: Clinical settings for K3 and K4 data collection	19
Table 2.3: Clinical settings for K5 data collection.....	19
Table 3.1: Numerical data for Figure 3.1.....	38
Table 3.2: Numerical data for Figure 3.2.....	39
Table 3.3: Numerical data for Figure 3.3.....	40
Table 3.4: Numerical data for Figure 3.4.....	41
Table 3.5: Numerical data for Figure 3.8.....	49
Table 3.6: Numerical data for Figure 3.9.....	50
Table 3.7: Numerical data for Figure 3.10.....	51
Table 3.8: Numerical data for Figure 3.11.....	52
Table 3.9: Numerical data for Figure 3.12.....	53
Table 3.10: Numerical data for Figure 3.13.....	54
Table 3.11: Numerical data for Figure 3.14.....	55
Table 3.12: Numerical data for Figure 3.15.....	56
Table 3.13: Numerical data for Figure 3.16.....	57
Table 3.14: Numerical data for Figure 3.17.....	58
Table 3.15: Numerical data for Figure 3.18.....	59

Table 3.16: Numerical data for Figure 3.19.....	60
Table 3.17: Numerical data for Figure 3.20.....	61
Table 3.18: Numerical data for Figure 3.21.....	62
Table 3.19: Numerical data for Figure 3.22.....	63
Table 3.20: Numerical data for Figure 3.23.....	64
Table 3.21: Numerical data for Figure 3.24.....	65
Table 3.22: Numerical data for Figure 3.25.....	66
Table 3.23: Numerical data for Figure 3.26.....	67
Table 3.24: Numerical data for Figure 3.27.....	68
Table 3.25 Distribution parameters	73

List of Figures

Figure 1.1: X-ray tube diagram.	3
Figure 1.2: A Philips Allura Xper FD20 system.....	5
Figure 2.1: Atom phantom family	15
Figure 2.2: Patient phantom setup.....	16
Figure 2.3: Experimental setup.....	2517
Figure 2.4: Exposure rates vs operator heights.....	20
Figure 2.5: Exposure rates vs measurement distance	21
Figure 2.6: Exposure rates vs contour shield use.....	22
Figure 2.7: Exposure rates for normal and cine modes	23
Figure 2.8: Exposure rates vs magnification level	24
Figure 2.9: Exposure rates for normal and low dose fluoroscopy	24
Figure 2.10: Exposure rates vs SID	25
Figure 3.1: Air kerma rates for biliary tube procedures	38
Figure 3.2: Air kerma rates for central line procedures.....	2539
Figure 3.3: Air kerma rates for gastro-/gastrojejunal procedures	40
Figure 3.4: Air kerma rates for nephrostomy tube procedures	2541
Figure 3.5: Machine utilization for Jul 2019–Jun 2020.....	42
Figure 3.6: Machine utilization for Jul 2020 -Jun 2021	43
Figure 3.7: Machine utilization for Aug 2021-Aug 2022.....	43
Figure 3.8: Operator air kerma rates for biliary tube procedures on K1	49
Figure 3.9: Operator air kerma rates for central line procedures on K1.....	50

Figure 3.10: Operator air kerma rates for gastro/gastrojejeunal tube procedures on K1..	51
Figure 3.11: Operator air kerma rates for nephrostomy tube procedures on K1	52
Figure 3.12: Operator air kerma rates for biliary tube procedures on K2	53
Figure 3.13: Operator air kerma rates for central line procedures on K2.....	2554
Figure 3.14: Operator air kerma rates for gastro/gastrojejeunal tube procedures on K2	2555
Figure 3.15: Operator air kerma rates for nephrostomy tube procedures on K2.....	56
Figure 3.16: Operator air kerma rates for biliary tube procedures on K3	57
Figure 3.17: Operator air kerma rates for central line procedures on K3.....	58
Figure 3.18: Operator air kerma rates for gastro/gastrojejeunal tube procedures on K3..	59
Figure 3.19: Operator air kerma rates for nephrostomy tube procedures on K3.....	60
Figure 3.20: Operator air kerma rates for biliary tube procedures on K4.....	61
Figure 3.21: Operator air kerma rates for central line procedures on K4.....	62
Figure 3.22: Operator air kerma rates for gastro/gastrojejeunal tube procedures on K4..	63
Figure 3.23: Operator air kerma rates for nephrostomy tube procedures on K4.....	64
Figure 3.24: Operator air kerma rates for biliary tube procedures on K5.....	65
Figure 3.25: Operator air kerma rates for central line procedures on K5.....	66
Figure 3.26: Operator air kerma rates for gastro/gastrojejeunal tube procedures on K5..	67
Figure 3.27: Operator air kerma rates for nephrostomy tube procedures on K5.....	68
Figure 3.28: Comparison of operator A fluoroscopy times for central line procedures. ..	69
Figure 3.29: Comparison of operator B fluoroscopy times for central line procedures. ...	69
Figure 3.30 Comparison of operator C fluoroscopy times for central line procedures.....	70
Figure 3.31: Comparison of operator D fluoroscopy times for central line procedures..	70

Figure 3.32: Comparison of operator E fluoroscopy times for central line procedures.	71
Figure 3.33: Comparison of operator F fluoroscopy times for central line procedures. ...	71
Figure 3.34: Comparison of operator G fluoroscopy times for central line procedures. ..	72
Figure 3.35: Comparison of operator H fluoroscopy times for central line procedures. ...	72
Figure 3.36: Comparison of operator I fluoroscopy times for central line procedures.	73
Figure 3.37: Yearly provider caseload breakdown for Jul 2019-Jun 2020.	75
Figure 38: Yearly provider caseload breakdown for Jul 3030-Jun 2021	75
Figure 3.39: Yearly provider caseload breakdown for Aug 2021-Aug 2022	76

Acknowledgements

I would like to first thank my advisors, Dr. Chu Wang and Dr. Terry Yoshizumi, for the opportunity to pursue this project as well as their consistent guidance and support throughout the evolution of this research.

This research would not have been possible without the previous work done by Dr. Robert Reiman and Dr. Steve Mann, who provided the historical data used in this thesis. I also appreciate the time and effort Dr. Mann spent supervising the practical portion of this research and sharing his fluoroscopy knowledge and expertise.

Lastly, I would like to thank the rest of my thesis committee, the Duke Radiation Dosimetry Laboratory staff, and Dr. Charles Kim for their invaluable perspectives and insights into this project

Chapter 1. Introduction

1.1 Interventional Radiology

Interventional Radiology (IR) is a medical specialty in which doctors diagnose and treat patients using image-guided, minimally invasive surgical procedures. These procedures involve the manipulation of small instruments such as needles, wires, and catheters inserted into the patient via an incision and subsequently threaded through the body to reach and treat specific organs or structures. Throughout this process the doctors are acquiring images as needed to visualize the path of their instruments and the progress of applicable treatment. Imaging modalities used for IR include fluoroscopy, ultrasound, computed tomography (CT), and magnetic resonance imaging (MRI). Benefits of IR include less pain, lower risk, and shorter recovery time for patients than traditional major surgery; however, it also exposes patients and operators to ionizing radiation when used with fluoroscopy and CT [1].

1.2 Fluoroscopy Guided IR

Of all the imaging modalities utilized for interventional procedures, fluoroscopy is by far the most common [2]. Fluoroscopy images are in essence series of individual projection x-ray images that are taken in quick succession by using a pulsed x-ray beam. To fully investigate the dynamic nature of IR, the imaging process and its relationship to both patient and operator dose must be understood.

1.2.1 X-ray production

When energetic electrons interact with matter, one mechanism by which they lose energy is through inelastic scattering. In this process, the Coulombic force between negatively charged electrons and positively charged nuclei of the matter cause deflection and deceleration of the electron. The energy lost by the electron in this process is released as an x-ray photon, referred to as Bremsstrahlung radiation, and is determined by the distance between the electron and the nuclei. Bremsstrahlung radiation is emitted with a spectrum of energies with a maximum value of the initial energy of the electrons.

Another type of x-ray that contributes to image formation is characteristic x-rays. An electron can be ejected from its atomic shell if it collides with an incident electron that exceeds its binding energy. This ejection creates a vacancy which will immediately be filled by an electron from an outer shell (if present). The transitioning electron will emit an x-ray photon whose energy is equal to the difference between the binding energies of the two shells. Characteristic x-ray production makes up a much smaller proportion of the total x-ray spectrum than Bremsstrahlung radiation.

1.2.2 X-ray tubes

Figure 1.1 is a simplified diagram of a modern x-ray tube. The high voltage source creates a large potential difference between the cathode and the anode. The cathode is negatively charged and contains a filament which is typically made of tungsten. When voltage is applied to the cathode, the filament wire becomes heated to a point where it

undergoes thermionic emission and electrons are freed from its surface. The free electrons are then accelerated away from the cathode and toward the positively charged anode. The x-ray tube is kept under a high vacuum seal to prevent the electrons from interacting with gas molecules as they move from the cathode to the anode.

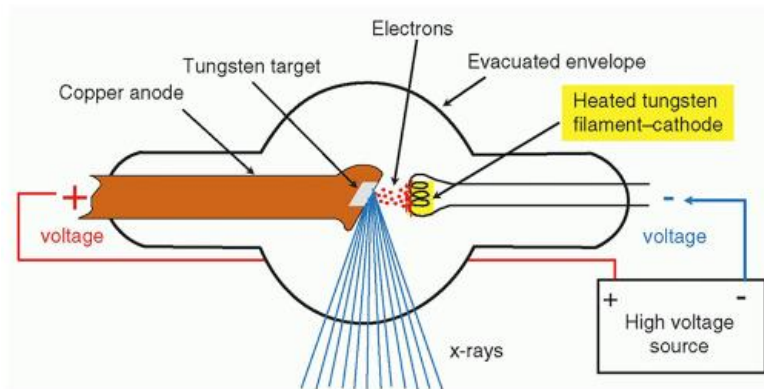


Figure 1.1: X-ray tube diagram. Image from Radiology Key [3]

In x-ray tubes used for fluoroscopy, the anode is an angled, rotating disk typically made of tungsten. It provides a target medium for the electrons from the cathode to interact with and create Bremsstrahlung radiation which is emitted in all directions. The tube is encased in a shielded housing, with a small port opening to allow x-rays which are emitted in a selected direction to leave the tube. These x-rays constitute the primary beam.

1.2.3 X-ray interactions with matter

Photon interactions in matter are probabilistic events. For the energy range used for fluoroscopy, the x-rays in the primary beam will interact with matter in one of two ways, either through the photoelectric effect or Compton scattering. The photoelectric

effect is more prevalent at lower energies when x-rays interact with atoms. In a photoelectric interaction, the x-ray imparts all its energy to an orbital electron and if the photon energy exceeds the binding energy of the electron, the electron will be ejected. The ejected electron will have an initial kinetic energy equal to the difference between the binding energy and the incident photon and will subsequently deposit this energy in the medium through charged particle interactions.

When it comes to interactions with human tissue, Compton scattering is the dominant mechanism of photon interaction at 75-125 kVp, the typical range of tube potentials used for fluoroscopy. A Compton event occurs when an incident photon interacts with an atom's outer shell electrons. The photon imparts a fraction of its energy to the electron as kinetic energy, freeing the electron. The reduction in energy causes the photon to change direction (scatters) as it continues through the medium, while the freed electron loses the imparted energy through charged particle interactions in the medium. Compton scattering is important in fluoroscopy because the patient acts as a scattering medium for the primary beam, and the scattered photons contribute additional noise to images and are the main source of occupational dose to operators [4].

Removal of photons from the primary beam due to absorption or scatter is called attenuation. Photons that are not attenuated will pass through the irradiated material without interacting at all. In this case, the photons will reach the detector and form an image. Although the beam generated by an x-ray tube is -poly-energetic, the distribution

of individual photons is relatively homogeneous except for gradations caused by the anode-heel effect. Attenuation differences in the body due to varying density and thickness of anatomical structures change the distribution of photons reaching the detector and results in greyscale differences in the final image.

1.2.4 Fluoroscopy Systems and Key Characteristics

Figure 1.2 shows an example of one of the interventional fluoroscopy models in use at Duke University Hospital (DUH), which includes a patient table, image display monitors, and a “C-arm” which holds the x-ray generator, x-ray tube, and a flat-panel digital detector. The detector is located opposite the x-ray tube and the distance between these two components can be adjusted as needed, although the range for this separation is limited based on the specific make and model of the system being used. The patient is placed between the tube and detector to allow for imaging during the procedures.



Figure 1.2: A Philips Allura Xper FD20 system with major components labeled. Image from Philips Healthcare [5]

IR operators use the images they acquire to guide their actions during procedures, so they need images of high quality to ensure they can properly visualize anatomical structures and their equipment. Additionally, the required image quality will vary depending on the procedure being done, the patient anatomy, and the projections used.

The main aspects of image quality in fluoroscopy are resolution, contrast, and noise. For the purposes of this study, resolution is not addressed and further use of the term “image quality” is meant to specify contrast and noise. Contrast is the difference in greyscale intensity between structures in an image. The greyscale intensity is related to the number of photons reaching a detector, so highly attenuating material will cause low intensities and high intensities will occur in areas of low attenuation. Good contrast is necessary to be able to visualize different structures in the body, and is achieved when there are large differences between the number of photons reaching the detector at any two points.

Noise is the variation of pixel intensities in an image and can have multiple sources. Electronic noise is an inherent property of the detection and image processing system and is therefore relatively constant and cannot be reduced by the actions of an operator. Anatomical noise is a property of the individual patients. This will remain relatively constant throughout a procedure and cannot be reduced unless digital subtraction methods are employed. Quantum noise is the most significant source of

noise in a fluoroscopy image and is related to the number of photons reaching individual pixels on the detector. Unlike electronic and anatomical noise, quantum noise fluctuates based on beam characteristics and can therefore be dynamically adjusted by changing the signal generated by the x-ray tube.

Because noise causes fluctuations in pixel intensities, it has a detrimental effect on contrast. A minimum contrast-to-noise ratio (CNR) is therefore needed to ensure fluoroscopy images are of good enough quality for IR purposes. To improve CNR, there are a number of ways that noise can be reduced without affecting contrast. One way this can be done by increasing the number of photons incident on the detector by increasing any combination of mA, pulse width, or number of pulses. These improvements in noise come at the cost of increasing radiation dose to the patient and operator. To maintain the balance between good image quality and low radiation doses, IR units are equipped with an Automatic Exposure Rate Control (AERC) circuit. This circuit consists of sensors which monitor photon fluence at the detector and send signals to the x-ray generator to adjust the beam to maintain a constant, pre-programmed Signal to Noise Ratio (SNR). Like their name implies, AERCs operate automatically, and the adjustments made to the beam can differ based on the protocol and operating mode selected, as well as the image processing algorithms employed by the unit.

Dose to the operator is in part a function of the number of photons incident on the operator and the energy those photons impart. It is caused by the fraction of photons

which undergo Compton scattering and whose resulting photon is scattered in the direction of the operator. The beams generated in fluoroscopy have a spectrum of energies, and the amount of energy lost when photons are scattered is also variable, so while scatter incident on the operator can have a wide range of energies it will never exceed the maximum energy of the primary beam. The variations listed above mean that while dose to an operator during an IR procedure cannot be directly calculated, it can be loosely linked to the Air Kerma (AK).

AK is the kinetic energy transferred from the incident photons per unit mass of air and is automatically measured on fluoroscopy units, typically at a point 15 cm from isocenter towards the x-ray tube. Changing the total number of photons passing through this point or their maximum energy will cause a change in AK, and we can anticipate that for similar scatter mediums with similar geometry and field size settings, changes in AK would cause certain changes to operator dose.

1.3 Occupational exposure limits and radiation protection in IR

In the State of North Carolina, occupational exposure to x-ray radiation is regulated by Chapter 15 “Radiation Protection”, Title 10A “Health and Human Services”, of the North Carolina Administrative Code (10A NCAC 15). Interventional radiologists at DUH who operated x-ray devices are categorized as radiation workers, and as such are subject to the annual exposure limits listed below.

Table 1.1: Annual occupational radiation dose limits

Whole body (Total Effective Dose Equivalent)	50 mSv
Any individual organ or tissue (Total Organ Dose Equivalent)	500 mSv
Lens of the Eye (Lens Dose Equivalent)	150 mSv
Skin of the Whole-body or any extremity (Shallow Dose Equivalent)	500 mSv
Embryo/Fetus of a Declared Pregnant Worker (Dose Equivalent)	5 mSv

These occupational dose limits are consistent with those defined by the United States Nuclear Regulatory Commission regulations in Part 20 “Standards for Protection against Radiation”, Title 10 “Energy”, of the Code of Federal Regulations (10 CFR 20) [6].

The occupational exposure for IR operators at DUH are monitored by dosimeters that are worn at the collar, outside their protective apron, and are typically processed on a monthly basis to ensure that personnel at risk for exceeding their annual limit will be identified and removed from the radiation environment prior to reaching 5 rem (50 mSv).

Radiation protection programs aim to protect personnel from harmful effects of exposure to radiation without limiting the benefits that come with radiation use and are a key component of radiation-related work environments. Workplace radiation protection practices focus on reducing occupational exposure to levels that are As Low

As Reasonably Achievable (ALARA), and the three key principles of doing so are time, distance, and shielding [7,8]. Radiation exposure is reduced when personnel lower the amount of time they are exposed; increase the distance between themselves and the radiation source; and utilize appropriate shielding. In the case of fluoroscopy-guided IR procedures, these principles are incorporated in clinical practice in three main ways: 1) minimizing the number of images taken, or the length of time the beam is on; 2) maximizing the distance between the x-ray tube and the patient, as well as between the patient and operators; and 3) utilizing protective shields, aprons, thyroid shields, glasses, and/or gloves. Time and shielding are especially important because IR operators actively perform invasive procedures including arterial embolization, nephrostomy tube placement and so forth during image acquisition, so the distance they can put between themselves and the source of their exposure is limited.

IR departments regularly balance large caseloads among a fixed number of operators, each of whom is limited on how much occupational exposure they can receive in a year. Optimization of individual provider exposure not only reduces the likelihood of operators exceeding their federal limits, which comes with negative consequences to the organization, but would also allow for maximization of caseloads within the occupational exposure limit of the staff as a whole.

1.4 IR at Duke University Hospital

Duke University Hospital (DUH) Interventional Radiology is a division of the Radiology Department. At the time of writing, DUH employs a faculty of 9 full-time IR operators, 15 residents who are in different stages of IR specialty training, 3 advanced practice operators (PA/NP), 15 IR technologists, and 14 IR nurses. Although DUH utilizes a variety of imaging modalities for IR procedures, this project will focus on the fixed fluoroscopy units.

Table 1.2: DUH IR system information

System Name	Manufacturer	Model	Available Filtration
K1	Philips	AlluraClarity Xper FD 20/20	0.1 mm Cu 0.4 mm Cu
K2	Philips	AlluraClarity Xper FD 20/15	0.1 mm Cu 0.4 mm Cu
K3	Philips	Allura Xper FD 20	0.1 mm Cu
K4	Philips	Allura Xper FD 20	0.1 mm Cu
K5	GE	Discovery IGS 740	0.1 mm Cu 0.4 mm Cu

The AlluraClarity FD 20/20 and FD 20/15 models are upgrades on the Allura Xper unit with two key differences: 1) the FD 20/20 and FD 20/15 units are bi-plane, and 2) the AlluraClarity models includes a software upgrade Philips calls ClarityIQ technology. The improvements included with ClarityIQ are explained in detail in the Philips ClarityIQ technology white paper [9], and ultimately result in units K1 and K2 being able to obtain images of similar quality as K3 and K4 with reduced dose to the

patient and operator. For the scope of this thesis, the lateral tube of the bi-plane units was not included. K5 is a GE Discovery IGS 740 which is a single C-arm unit.

1.5 Challenges in evaluating radiation dose to operators

The beam in a fluoroscopy machine is one-directional and well-collimated, and the x-ray tube is shielded to minimize radiation leakage. Because of this, the main source of radiation exposure to operators is scatter radiation resulting from the primary beam interacting with body tissues in the patient [10]. Scatter radiation arises from probabilistic mechanisms such as Compton scatter and is emitted in directions that are determined by the energy and direction of the primary photons, the effective atomic numbers of the body tissues and other factors. This, along with the automatic adjustment of beam parameters throughout procedures, makes occupational exposures to operators highly variable and difficult to evaluate without dosimeter data.

1.6 Goals

The goal of this project is to develop tools which can be used by interventional radiology departments to assess or improve clinical dose reduction methods. This is done in two parts: contextualizing local operator dose and developing a conceptual framework for self-assessment of differences between case performance and the potential impact on operator dose.

In Chapter 2, an experimental setup tests the effect on occupational dose of changing specified parameters while using clinical machine settings. The effects of these

changes on dose from the primary beam are well described by physical principles, and the measured data aimed to describe the relationship between these changes and the dose that operators receive from scatter radiation.

Chapter 3 proposes an initial framework to use historical procedure data to identify trends in performance that can affect operator dose. This framework focuses on identifying metrics within RDSR data that can be accurately compared and linked to differences in occupational dose among staff members.

Chapter 2. Measuring the Effects of Changing Clinical Settings on Operator Dose

2.1 Introduction

The success of occupational radiation safety programs relies on the actions of the participants. Improvement of these programs must therefore address the behaviors and attitudes of the staff in their day-to-day work. Personnel receive training on radiation protection measures related to their jobs, but implementation of these measures is solely up to the individuals and can be inconsistent across a group of peers performing the same work. Consistency in utilizing dose reduction methods is especially important for IR operators due to the high doses they receive.

One way to motivate staff to increase their consistency in implementing dose reduction techniques is to emphasize the benefit of individual techniques. The following experiment was designed to test the relationships between specific fluoroscopy variables and operator dose. IR operators receive radiation safety training throughout their careers and are aware of the basic effects on dose that some techniques offer, but the results from this experiment can give a better idea of the magnitude of dose reduction available and lead to more consistent prioritization of these techniques by operators.

2.2 Materials and Methods

2.2.1 Phantom Setup and Shielding

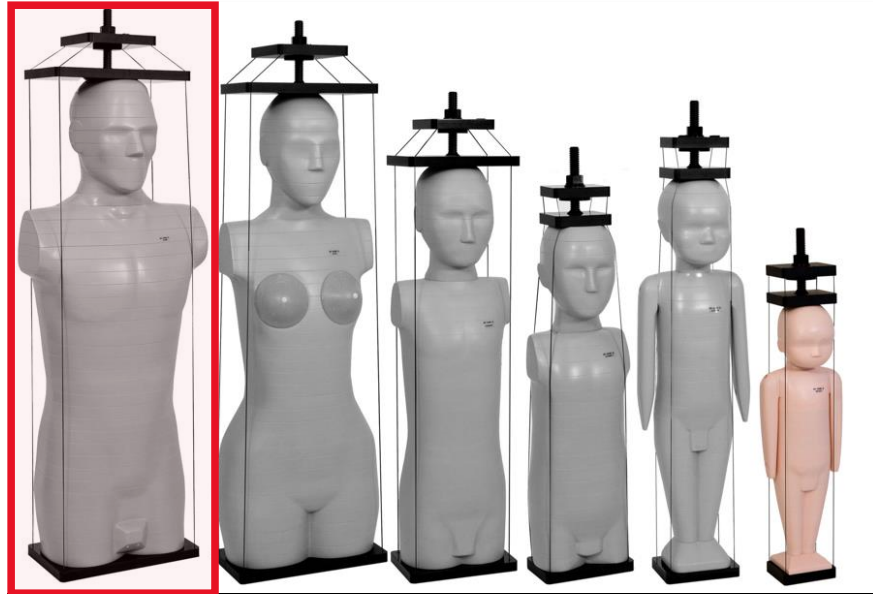


Figure 2.1: Image of Atom phantom family [11] with the male phantom indicated by the red box.

Two phantoms were used for this experiment. The “patient” phantom consisted of a 5-gallon water jug (diameter 9 inches) wrapped in 1.5 inches of fat-equivalent material for a total diameter of 12 inches. The “operator” phantom was the Atom Dosimetry Labs (Norfolk, VA) Adult Male phantom indicated in Figure 2.1. For each IR unit, the C-arm was positioned with the x-ray tube located below the table as seen in Figure 2.2. The patient phantom was placed on the table and centered in the field of view (FOV), with the table height adjusted to achieve a SOD of 24.5 inches. The operator phantom was placed on a cart positioned at the side of the table and draped with a lead apron. A Ludlum 9DP Pressurized Ion Chamber, SN: 25015676, was placed on foam

blocks directly in front of the operator phantom at collar-level. The cart was positioned so the center markings of the ion chamber were 15 inches lateral to and 25 inches inferior from the center of the flat-paneled detector. This position was chosen to mimic a normal orientation between a patient and operator. A correction factor of 1.05 was applied to the readings from the ion chamber based on calibration data.



Figure 2.2: Patient phantom setup



Figure 2.3: Full experimental setup with contour shield in place

2.2.2 Clinical Parameters and Variables

A general abdomen protocol was selected, and dose measurements were taken at settings defined in Table 2.1 for K1 and K2, Table 2.2 for K3 and K4, and Table 2.3 for K5. The specific frame rates in frames per second (fps) and available field sizes differed based on the unit model, however care was taken to select “like” settings across the units. For example, the 12.5 fps - M mode and the 15 fps - N mode are the “Fluoro II” settings on the respective units for the selected protocol.

The settings selected for this experiment were chosen to measure the effect specific variables had on the operator dose compared to a reference measurement. Operator phantom height was changed to determine whether height differences affected recorded doses based on the change in dosimeter location. Contour shield effectiveness

was investigated because it is a dose reduction method available for all systems and operators but may not always be used. Fluoroscopy mode, SID and magnification are all settings that can be implemented by the operator and can affect operator dose. Ideally operators would use the lowest dose settings and adjust as needed based on the needed image quality.

A separate set of measurements were taken to evaluate the effectiveness of the contour shield. The settings from Technique #1 were used to take three 5-minute shots with the contour shield in place, and three 30-second shots without the contour shield.

Table 2.1: Clinical settings for K1 and K2 data collection

Technique #	Operator Phantom Height (in)	Mode	Contour Shield Used	SID (cm)	Magnification Used	FOV (mm)	Irradiation Time (s)
1	64	12.5 fps - M	No	120	None	380x300	30
2	70	12.5 fps - M	No	120	None	380x300	30
3	70	12.5 fps - M	Yes	120	None	380x300	30
4	70	12.5 fps - M	No	120	Yes	190x190	30
5	70	6 fps - Cine	No	120	None	380x300	10
6	70	12.5 fps - L	No	120	None	380x300	30
7	70	12.5 fps - M	No	110	None	380x300	30
8	76	12.5 fps - M	No	120	None	380x300	30

Table 2.2: Clinical settings for K3 and K4 data collection

Technique #	Operator Phantom Height (in)	Mode	Contour Shield Used	SID (cm)	Magnification Used	FOV (mm)	Irradiation Time (s)
1	64	15 fps - N	No	120	None	380x300	30
2	70	15 fps - N	No	120	None	380x300	30
3	70	15 fps - N	Yes	120	None	380x300	30
4	70	15 fps - N	No	120	Yes	190x190	30
5	70	6 fps – Cine	No	120	None	380x300	10
6	70	15 fps - L	No	120	None	380x300	30
7	70	15 fps - N	No	110	None	380x300	30
8	76	15 fps - N	No	120	None	380x300	30

Table 2.3 Clinical settings for K5 data collection

Technique #	Operator Phantom Height (in)	Mode	Contour Shield Used	SID (cm)	Magnification Used	FOV (mm)	Irradiation Time (s)
1	64	15 fps - Normal	No	120	None	400x400	30
2	70	15 fps - Normal	No	120	None	400x400	30
3	70	15 fps - Normal	Yes	120	None	400x400	30
4	70	15 fps - Normal	No	120	Yes	200x200	30
5	70	7.5 fps - Cine	No	120	None	400x400	10
6	70	15 fps – Low Dose	No	120	None	400x400	30
7	70	15 fps - Normal	No	110	None	400x400	30
8	76	15 fps - Normal	No	120	None	400x400	30

2.3 Results

Results are reported in units of exposure, Roentgen. Absorbed dose from exposure is calculated by multiplying exposure by a conversion factor called the F-factor. In certain radiation protection practice, conversion factor between exposure from photons with the energies used in fluoroscopy is taken to be 1 so although the following results are reported in Roentgen, they are considered to be equivalent to absorbed dose values [12].

2.3.1 Provider Height

Figure 2.4 shows the measured exposure rates from techniques 1, 2, and 8 for each unit.

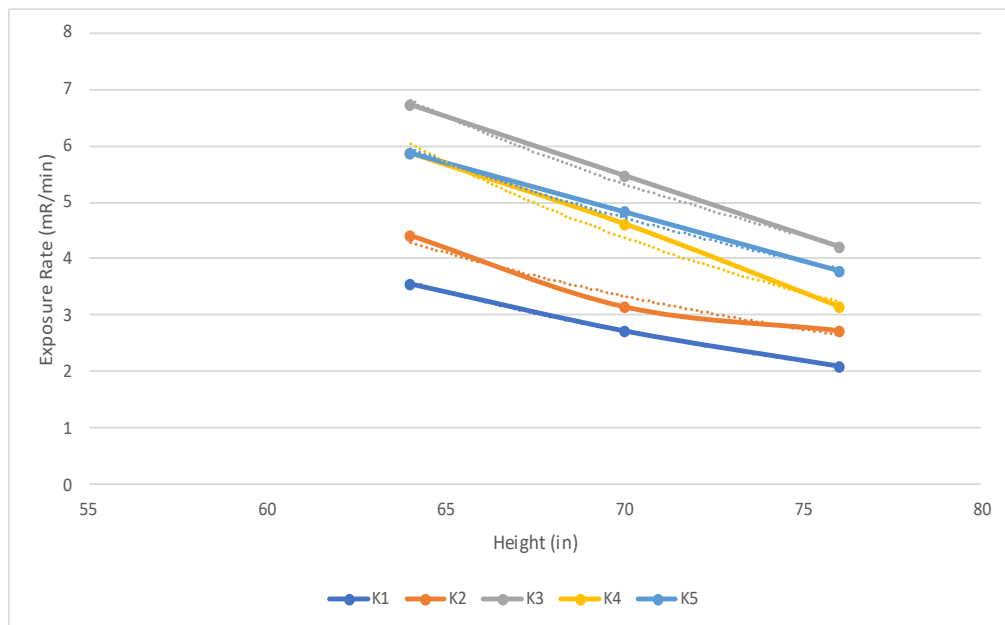


Figure 2.4: Exposure rates as a function of operator phantom height

Figure 2.5 shows the measured exposure rates from techniques 1, 2, and 8 for each unit as a function of direct distance from the phantom to the measurement point (ion chamber).

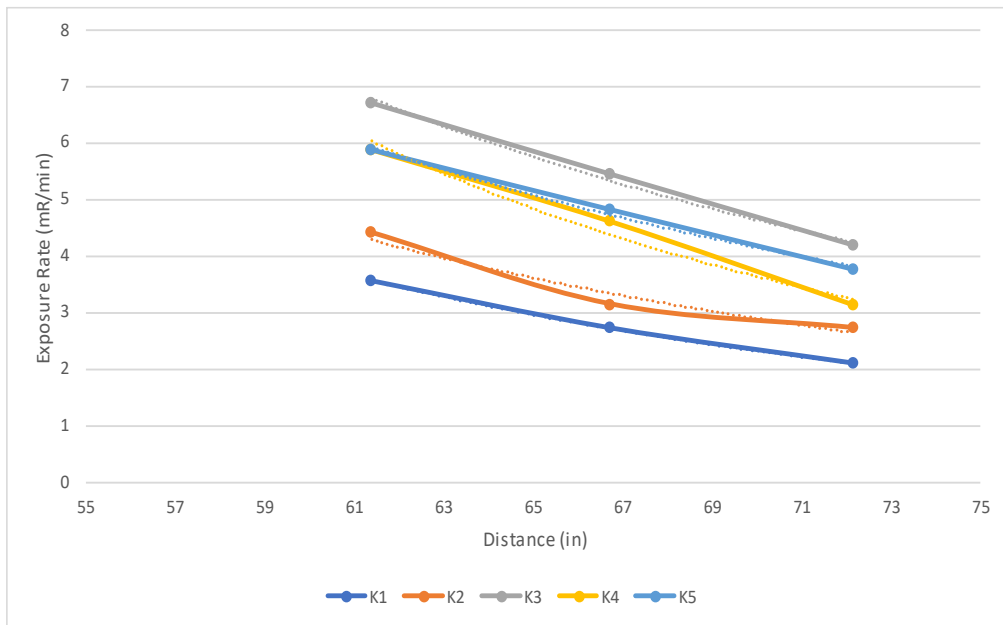


Figure 2.5: Exposure rates as a function of distance between patient phantom and measurement point

2.3.2 Contour shield use

Figure 2.6 shows the measured exposure rates for each unit from techniques 2 and 3 which were taken with and without the contour shield placed between the patient phantom and the ion chamber.

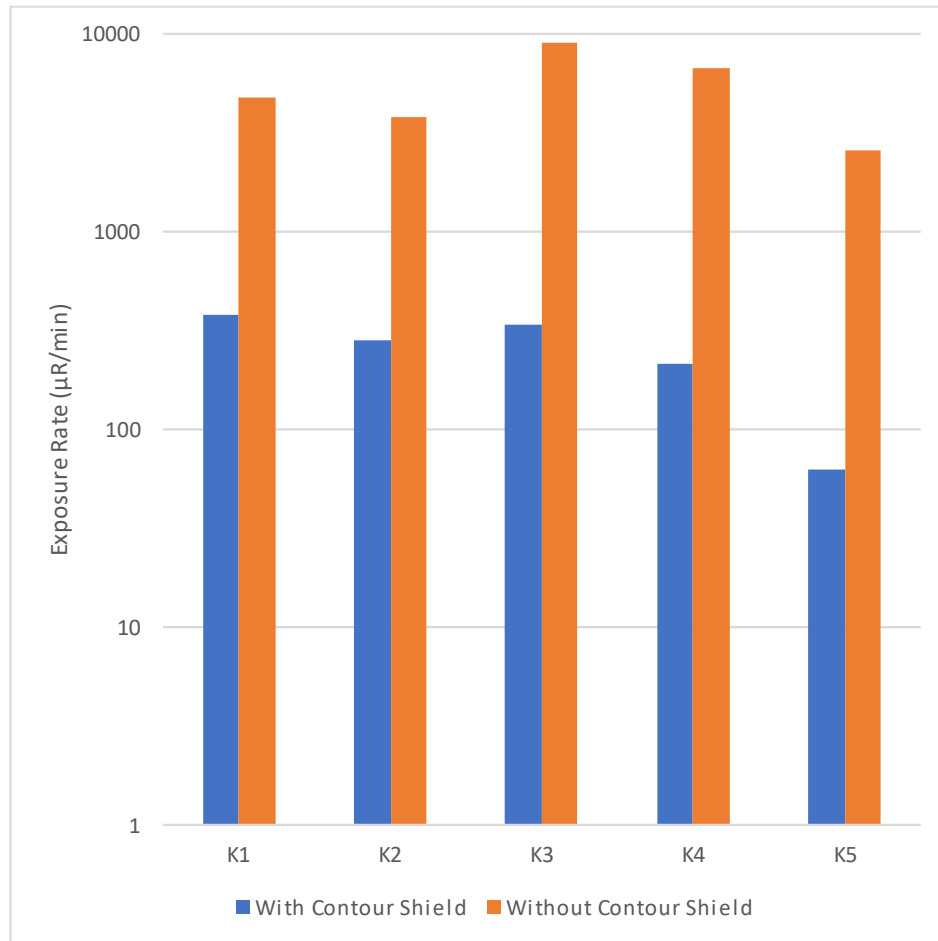


Figure 2.6: Exposure rates with and without contour shield

2.3.3 Cine Mode

Figure 2.7 shows the measured exposure rates for techniques 2 and 5, the variation between the selected fluoroscopy and cine settings.

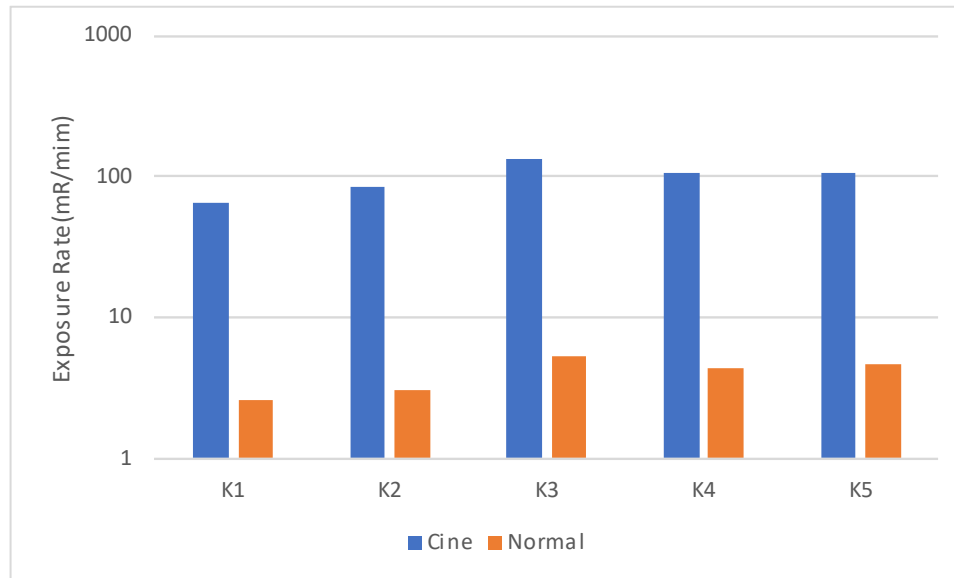


Figure 2.7: Exposure rates in cine and normal modes. Cine mode used 6 fps for K1-K4 and 7.5 fps for K5. Fluoroscopy mode used 12.5 fps for K1 and K2 and 15 fps for K3-K5.

2.3.4 Magnification

Figure 2.8 shows the measured exposure rates for techniques 2 and 4 which were done with the full FOV and the magnification indicated in tables 2.1 through 2.3.

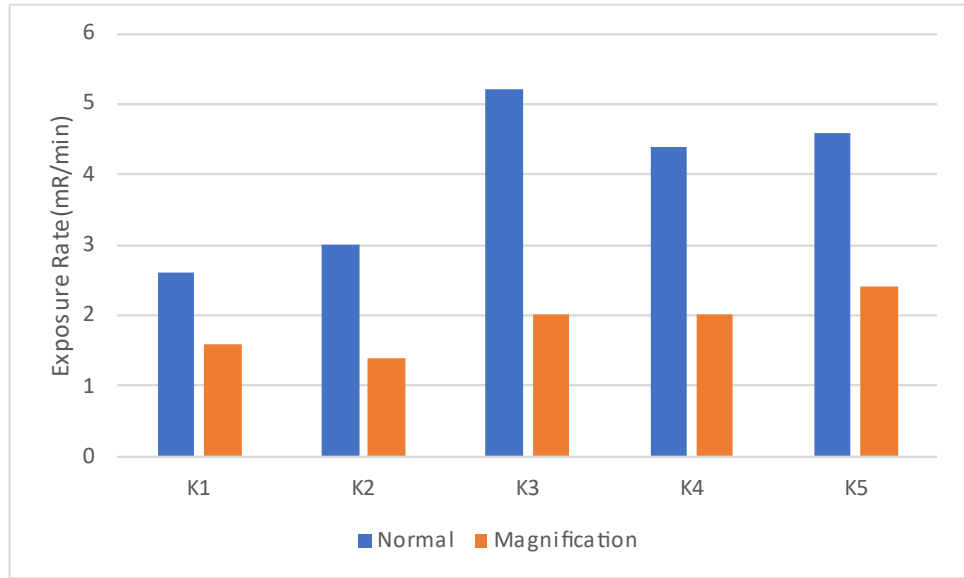


Figure 2.8: Exposure rates with and without magnification

2.3.5 Low Dose Mode

Figure 2.9 shows the measured exposure rates for techniques 2 and 6, the normal and low dose fluoroscopy modes for each unit.

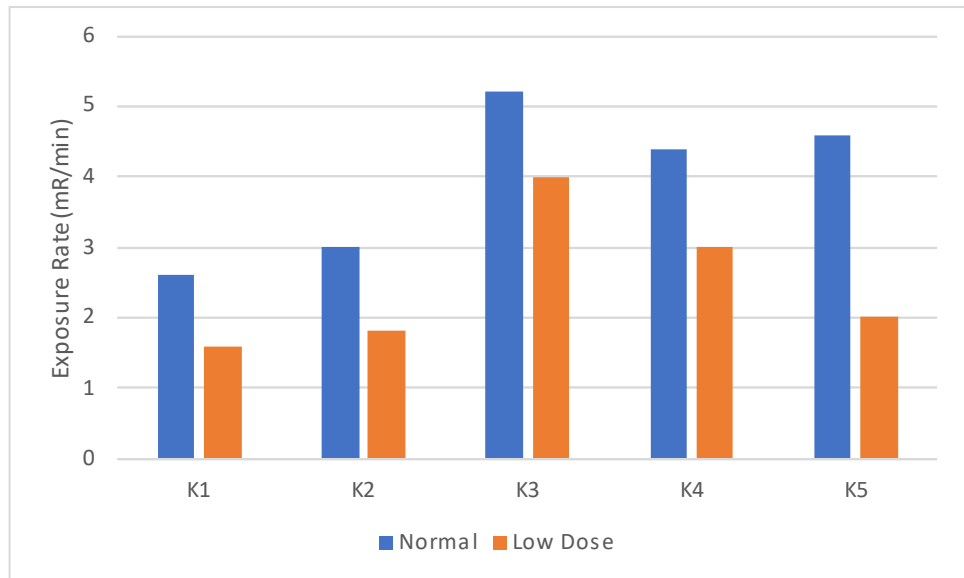


Figure 2.9: Exposure rates in normal and low dose modes

2.3.6 SID

Figure 2.10 shows the measured exposure rates for techniques 2 and 7 on units K1, K2, and K5, which were done with the SID set at 120 cm and 110 cm.

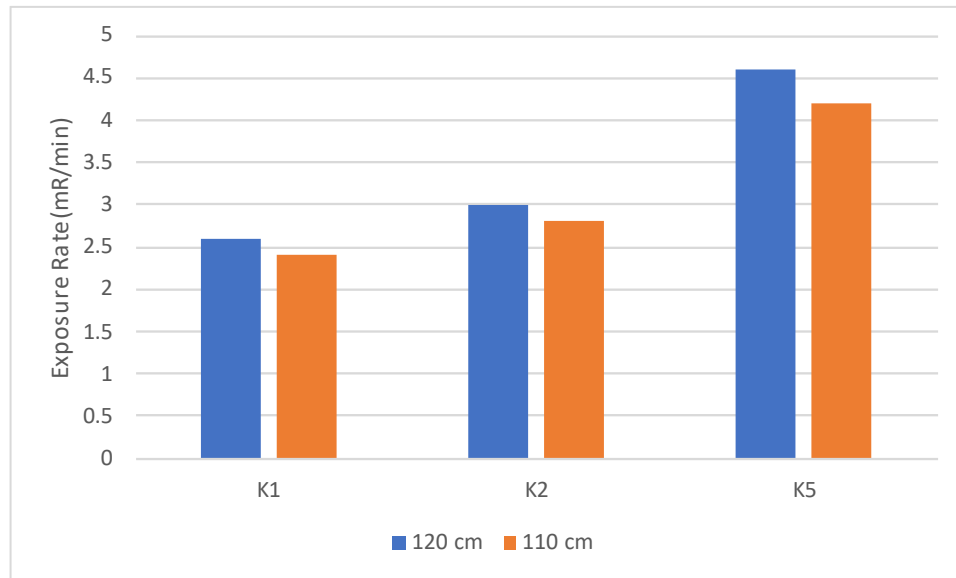


Figure 2.30: Exposure rates at 110 cm and 120 cm SID

2.4 Discussion

2.4.1 Provider Height

The well-known “inverse square law” is one of the most fundamental relationships in radiation protection and is the basis for utilizing distance to reduce radiation exposure. The inverse square law is part of the basic training that radiation workers are given but is based on a point source of radiation. Exposure to fluoroscopy operators is a distributed source dependent on beam characteristics, the field of view, and the thickness of the patient, therefore it cannot be predicted exactly by the inverse square law but does imply that there is an inverse relationship between operator

exposure and distance to the patient. Since IR operators wear their primary dosimeter at their collar, it's possible to have significant changes in measured dose between operators of different heights. Figure 2.4 shows the recorded exposure as a function of operator height. A power curve was fit to the data and the equations for each line are listed. The measured exposure was found to drop off slightly more quickly than predicted by the inverse square law. Instead of being proportional to the inverse square of the distance, the power exponential of the measured data's dependence on operator height was found to range from -2.5 to -3.6.

Although relating the change in measured dose to the change in operator height is practical information for the clinicians, it is prudent to note that because the operator is standing at an angle from the source of the scatter, a change in dosimeter height does not translate to the same amount of change in the true distance from the source of scatter to the dosimeter. The distance from the dosimeter to the center of the phantom at the plane of the tabletop was calculated for the three heights. The six-inch change in dosimeter height corresponded to a 5.3 to 5.4-inch difference in direct distance, and these distances are plotted with the measured exposures in Figure 2.5 and fit with power curves. Because the direct distance was smaller than the six-inch height change, the power exponential of the decrease in measured exposure had a larger magnitude, ranging from -2.9 to -3.8.

In clinical applications, it is more practical to relate dose difference to operator height. These results show that the change in dose rate to the operator for each 6-inch change in height varies between the five units. A six-inch change in height reduced exposure rates to operators by up to 30%, and a 12-inch change in height reduced exposure rates to operators by up to 45%. The exposure rates seen in this experiment correspond to fairly low operator dose rates, but as mentioned above operator dose can accumulate to a significant amount due to the number of procedures done and the amount of fluoroscopy used over a monitoring period. With such large cumulative dose, 30%-45% differences in exposure rates can cause a wide range of operator doses even with similar caseloads and fluoroscopy usage.

2.4.2 Contour Shield Use

The second variable examined was the effectiveness of using a contour shield during procedures. Initial data was taken with 30-second exposures however it was quickly noted that with the contour shield placed between the patient phantom and the ion chamber, the automated scale used on the ion chamber was too high to accurately measure the cumulative exposure over the 30-second period. To correct for this, a second set of measurements was taken using 5-minute exposures when the contour shield was in place, and 30-second exposures with no shielding. The corresponding exposure rates are shown in Figure 2.6. Contour shield use reduced the exposure rate to the operator by over 90% on all units. It's also interesting to note that even though K3

and K4 generally give higher exposures than K1 and K2, use of the contour shield brings the exposure rate to the operator down to a more equal level across the four units.

Contour shields are installed in each of the IR suites, however use by the operators is intermittent for a few reasons. There are some procedures where it is impossible to use the shield and still adequately reach the patient due to other necessary medical equipment being hooked up to the patient. There is also a difference in the reach and angles of each contour shield because of differences in room size, installation location, and equipment setup which can make using a shield more or less feasible for one unit compared to the others. Lastly, there are times when the operator simply forgets or chooses not to use the shield. Of the reasons listed for not using the contour shield, this is the only one that can be reasonable improved upon. Since the contour shield can reduce operator exposure by more than 90%, promoting and enforcing its use whenever possible is a simple and very effective way to minimize overall dose to staff.

2.4.3 Cine Mode

During cine acquisition, a cinematic recording is made of the fluoroscopy images as they are generated. Figure 2.7 shows the exposure rate to operators from normal fluoroscopy and cine modes. For all five units, the ratio of measured exposures matches closely to the ratio of AK for those exposures (within 3% in each case). The cine exposure also follows a similar pattern across the units as the fluoroscopy exposure. It is important for operators to understand the magnitude of the difference between cine and fluoroscopy

acquisitions. With such high exposure rates, overuse of cine can drastically increase their occupational exposure and can also contribute to a higher dose to patients.

2.4.4 Magnification

Each of the IR units had multiple magnification field sizes, and the field size corresponding most closely to one-half of the full field of view was chosen for this measurement. When using magnification, two processes can decrease the SNR compared to using a full FOV. First, many units will combine sets of individual detector elements into each pixel when using a large FOV, called binning. This slightly reduces the spatial resolution, but it increases the photon fluence across individual pixels by a factor equal to the number of detector elements binned together. As the field size reduces when magnification is employed, the number of detector elements comprising each pixel also reduces until binning no longer occurs. Each time the number of binned detectors is reduced, the SNR also reduces if the exposure rate is left unadjusted. The other factor to take into consideration is the noise perception. As the images are magnified so are the effects of the perceived noise, and a higher signal is needed to reduce these effects.

An expected boost in signal to balance out the effects noted above can be seen in the increased AK for the magnified techniques. The overall dose to the operators is significantly reduced by the collimators limiting the primary beam to a smaller area. Not only is the amount of scatter generated reduced by irradiating a smaller volume, but the

scatter also originates closer to the center of the phantom and is more likely to be attenuated by the portion of the phantom outside the FOV than to escape and contribute to operator dose.

The scatter reduction from decreasing the FOV more than balances the increased signal required to overcome excess noise in magnification mode, leading to the decrease in operator dose seen in all five units. This reduction is greater on K3 and K4, which may be caused in part by differences in filtration creating different beam and scatter profiles for these two machines. The extent to which kVp and mA settings play a role in this reduction would require further investigation since this data wasn't obtained in this experiment.

Because of the greater reduction for K3 and K4, use of magnification lowers the exposure rates to the operator to a level that is more consistent across the units than the exposure rates with a full FOV. While this is beneficial compared to utilizing full FOV imaging, this benefit must be balanced with the negative effects of giving higher doses to patients while using magnification. A good compromise for this goal would be for operators to use manual collimation which would reduce the FOV and scatter to the operator without the automatic increase of AK causing increased dose to the patient.

2.4.5 Low Dose Mode

Each of the IR units at DUH has three modes of operation within selected protocols. While they are labeled differently on each model, the modes correspond to a

low, “normal”, and high dose mode for the applied settings. The purpose for having different modes is to allow operators to select the lowest dose settings needed for the patient and procedure in question thereby minimizing patient and scatter dose. If the programmed AERC response at one setting is not providing sufficient image quality, such as for larger patients, the operator can then select the next higher dose mode.

For the protocol used in data collection, each unit uses the same amount of filtration in both the low and medium dose modes, but the amount of filtration is not consistent across all the units. As can be seen in Figure 2.9, the measured doses in both low and normal modes for K3 and K4 are higher than the other units. This is partly due to K3 and K4 having only 0.1 mm of copper filtration for this protocol while the other three units each use 0.4 mm copper. Even though the filtration levels are different, the constant filtration level between low and normal dose modes means the AERC adjustments are limited to kV, mA, and pulse duration. The measured dose reduction to operators when switching from normal to low dose mode was 23%-40% in the Philips units (K1, K2, K3 and K4) and roughly 57% in the GE unit (K5).

Use of the different dose modes available is a choice that the operator must make using his or her professional judgment of the attainable image quality. To maximize use of low dose modes, operators must have a robust knowledge of the available features on each unit and how to implement them. Quantifiable knowledge of the benefits of these features is also a key part of ensuring they are used. Since the lower dose modes offer

relatively poorer image quality, operators who are not aware of the implications to dose may consistently choose the mode offering the highest image quality at the expense of a higher-than-necessary radiation exposure, while imaging techniques with lesser image quality may also accomplish the clinical goals of the procedure. Thorough training and emphasis on utilizing these features can help maximize their implementation by individual operators, and lower overall dose received by both IR staff and their patients, while still fulfilling the clinical mission.

2.4.6 SID

In radiography, presence of an air gap between the patient and the detector was studied as a method of reducing scatter at the detector. The principle behind this concept is similar to that of the inverse square law where the increased distance would cause a reduction in the amount of scatter reaching the detector. In fluoroscopy, an air gap has a different effect. The drop in photon fluence at the detector from an air gap results in the AERCs boosting the signal to maintain target exposure at the detector and therefore increasing the patient and operator doses.

With C-arm units, the maximum distance between the x-ray tube and detector is limited based on the manufacturer and model. With the chosen table height and the diameter of the patient phantom, the maximum air gap achievable across all five fluoroscopy systems was 10 cm. Figure 2.10 shows the measured exposure rates with a 10 cm change in air gap distance, and a 7-9% reduction in exposure rate was seen on

units K1, K2, and K5 when the gap between the detector and patient phantom was shortened. This technique was performed with the anti-scatter grid in place on each unit, so differences in scatter will be system-specific, however when this technique was performed on K3 and K4 the measured decrease was much larger than what was seen on the other three units. Upon investigation, it was discovered that when acquiring data on K3 and K4, although the unit display indicated the collimators were open to the full FOV, the RDSR showed the field sizes for K3 and K4 were collimated by 5 cm on each edge. This happened because the collimators were opened to the full FOV before lowering the detector to the 110 cm SID, and they did not automatically adjust to the difference in the FOV due to the changed geometry. This caused additional dose reduction that was unanticipated on K3 and K4, and for that reason the acquired data for those units was omitted.

Chapter 3. Conceptual Framework for Analyzing the Radiation Dose Structured Report (RDSR)

Occupational dose in individual procedures can vary based on any combination of beam characteristics, patient and x-ray tube geometry, and the clinical practices of the operator. Utilizing historical RDSR data, procedure types were grouped together into four main categories for analysis based on anatomic and clinical similarities: biliary tube procedures, central line procedures, gastro-/gastrojejunal tube procedures, and nephrostomy tube procedures. All remaining procedure types were collectively categorized as “Other Procedures”. The procedures in each category are expected to have similar patient and x-ray tube geometry and to be performed using the same protocol. Under the same protocol and geometry, there would be some variation in exposure rates between individual procedures due to differences in patient thickness and the achievable SID. With large sample sizes ranging from 400-1400 procedures for each category, the fluctuations in patient size end up having little effect on the average, and differences in beam characteristics across individual cases are treated as independent of patient size.

3.1 Machine-Specific Differences

DUH utilizes five fixed interventional systems which include three different models from two manufacturers. Manufacturers make use of proprietary design and software in an attempt to provide the best product, and even within the same company

there can be significant differences between models. Hill et al [13] studied these types of variability among different manufacturers and generations of interventional units for pediatric cardiac catheterization and found that for similar protocols there were meaningful differences in dose and image quality between systems. This not only highlights the importance of institutions identifying and measuring these differences as done in Chapter 2 but also reinforces the foundational differences that must be accounted for before assessing operator differences.

When addressing machine-specific difference, air kerma rate (AKR) was used as the metric of comparison instead of the Dose Area Product (DAP), which is more conventionally used when assessing operator dose from fluoroscopy. AKR is a measure of the beam intensity and is dependent on characteristics which are adjusted in pre-programmed ways based on the selected protocol and the software in use on specific models. Unlike DAP, AKR is independent of field size and total fluoroscopy time which both can change based on the preference and needs of the operator. Fluoroscopy AKRs were compared across the procedure categories for all five IR units to determine any differences in output between the units for the same procedure types.

Once machine output trends are determined, the next step in addressing radiation dose to operators is to look at the cases that are being performed on each unit. The total exposure to IR operators as a group during a reporting period will be the sum of the doses from individual procedures performed in that time. In an ideal situation,

the procedures would be split among the operators so that everyone received an equal fraction of the total dose instead of some receiving higher doses and some receiving lower doses. In practice, there are limitations to scheduling such as machine availability, procedure fluoroscopy requirements, and operator experience. Nevertheless, if there are noticeable differences in machine outputs that can affect occupational doses, it would be beneficial for an IR department to evaluate the distribution of cases between the units and determine whether scheduling of procedures could be optimized by actively scheduling routinely higher-dose procedures on systems with lower average exposure rates.

3.1.1 Materials and Methods

For the following analysis, data was obtained from the RDSR for procedures performed by the IR operators at DUH. For each of the sources of variation listed above, the RDSR data was organized into subsets and compared based on selected metrics. The data was also subdivided into three 12-month periods: 01 July 2019 – 30 June 2020 (Year 1), 01 July 2020 – 30 June 2021 (Year 2), and 23 August 2021 – 22 August 2022 (Year 3). All analysis was done using Microsoft Excel and XLSTAT, a statistical analysis add-on for Excel.

3.1.1.1 Machine Performance

Utilizing data from Year 3, the fluoroscopy AKR was calculated for individual procedures by dividing the cumulative fluoroscopy AK by the total fluoroscopy time for

that case, and this was converted to units of mGy/min. For each procedure category, the fluoroscopy AKRs were organized into tables with columns representing the cases performed on an individual unit. This data was analyzed using XLSTAT's Descriptive Statistics function.

3.1.1.2 Machine Utilization

The total number of procedures performed on each unit for each year was counted for each procedure category. This data was then used to create percentage stacked column charts for each unit showing the year-to-year utilization proportion of each machine for the different procedure categories.

3.1.2 Results

3.1.2.1 Machine Performance

Figures 3.1 through 3.4 are box plots which show the variation of fluoroscopy AKRs for each procedure category across all five units. The key elements for this study are the green boxes indicating the inter-quartile range (IQR), or the values which fall within the dataset's 25th and 75th percentiles and the median which is indicated by the solid black line through each box. For all four categories, the median and IQR of fluoroscopy AKR values for K3 and K4 are higher than the other units. K1, K2, and K5 generally have similar median fluoroscopy AKR, but K5 has a larger IQR compared to K1 and K2.

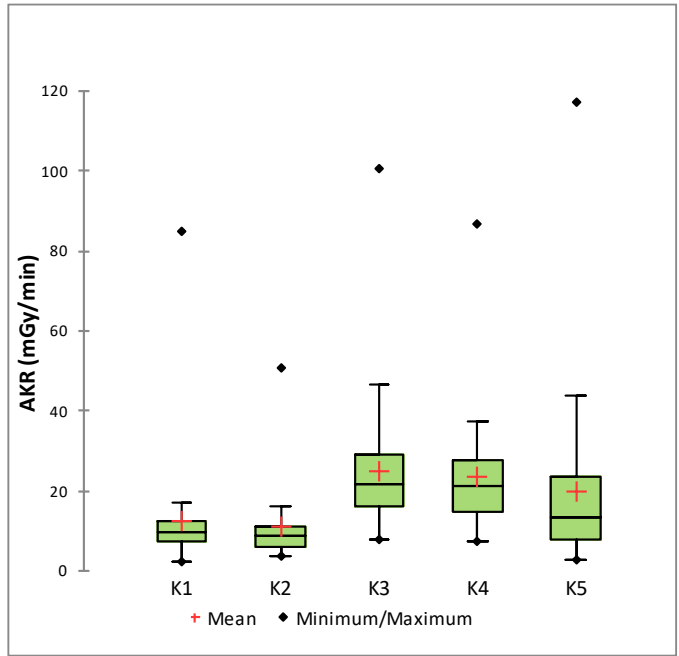


Figure 3.1: Comparison of historical AKRs for biliary tube procedures from Aug 2021-Aug 2022

Table 3.1: Numerical data for Figure 3.1

	K1	K2	K3	K4	K5
Number of Procedures	92	37	148	84	60
AKR Statistic (mGy/min)					
Minimum	2.16	3.50	7.96	7.17	2.60
Maximum	84.85	50.87	100.81	86.58	117.33
1st Quartile	7.50	5.85	15.98	14.90	7.79
Median	9.71	8.61	21.66	21.09	13.46
3rd Quartile	12.28	10.93	28.97	27.74	23.49
Mean	12.25	10.85	24.82	23.58	19.93

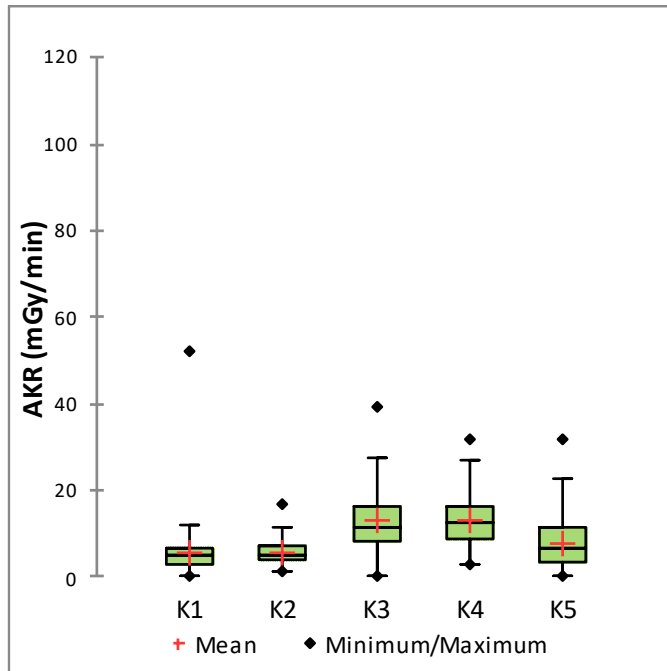


Figure 3.2: Comparison of historical AKRs for central line procedures from Aug 2021-Aug 2022.

Table 3.2: Numerical data for Figure 3.2

	K1	K2	K3	K4	K5
Number of Procedures	263	208	483	248	174
AKR Statistic (mGy/min)					
Minimum	0.20	1.44	0.00	3.13	0.00
Maximum	52.07	16.54	39.16	31.82	32.04
1st Quartile	3.03	3.81	8.40	8.90	3.25
Median	4.84	5.08	11.71	12.70	6.59
3rd Quartile	6.73	7.03	16.19	16.25	11.35
Mean	5.70	5.67	13.21	13.17	7.86

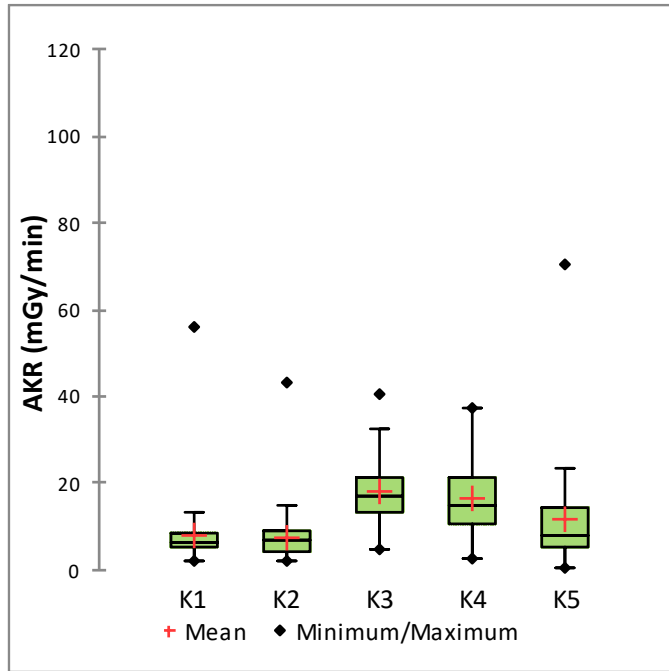


Figure 3.3: Comparison of historical AKRs for G/GJ tube procedures from Aug 2021-Aug 2022

Table 3.3: Numerical data for Figure 3.3

	K1	K2	K3	K4	K5
Number of Procedures	141	126	247	157	101
AKR Statistic (mGy/min)					
Minimum	2.18	1.92	4.55	2.70	0.39
Maximum	56.26	43.43	40.68	37.44	70.39
1st Quartile	5.07	4.39	13.43	10.51	5.10
Median	6.44	6.65	17.02	14.90	7.98
3rd Quartile	8.50	8.74	21.18	21.51	14.29
Mean	8.05	7.23	17.89	16.40	11.75

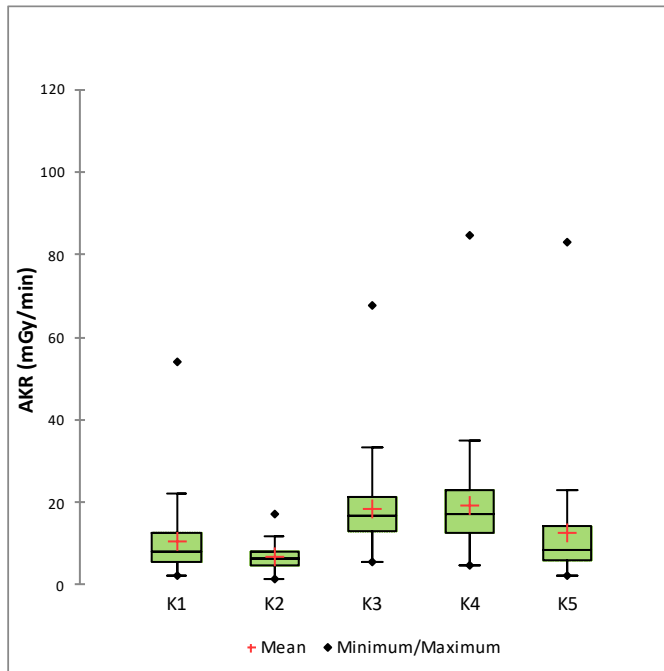


Figure 3.4: Comparison of historical AKRs for nephrostomy tube procedures from Aug 2021-Aug 2022

Table 3.4: Numerical data for Figure 3.4

	K1	K2	K3	K4	K5
Number of Procedures	133	79	190	92	54
AKR Statistic (mGy/min)					
Minimum	2.18	1.40	5.63	4.60	2.27
Maximum	54.10	17.09	67.79	84.60	83.23
1st Quartile	5.74	4.69	13.12	12.83	5.96
Median	8.07	6.39	16.59	17.17	8.37
3rd Quartile	12.45	8.15	21.48	22.87	14.40
Mean	10.69	6.69	18.63	19.40	12.78

3.1.2.2 Machine Utilization

Figures 3.5 through 3.7 show the yearly number of procedures performed on each unit, as well as the proportions of each procedure category.

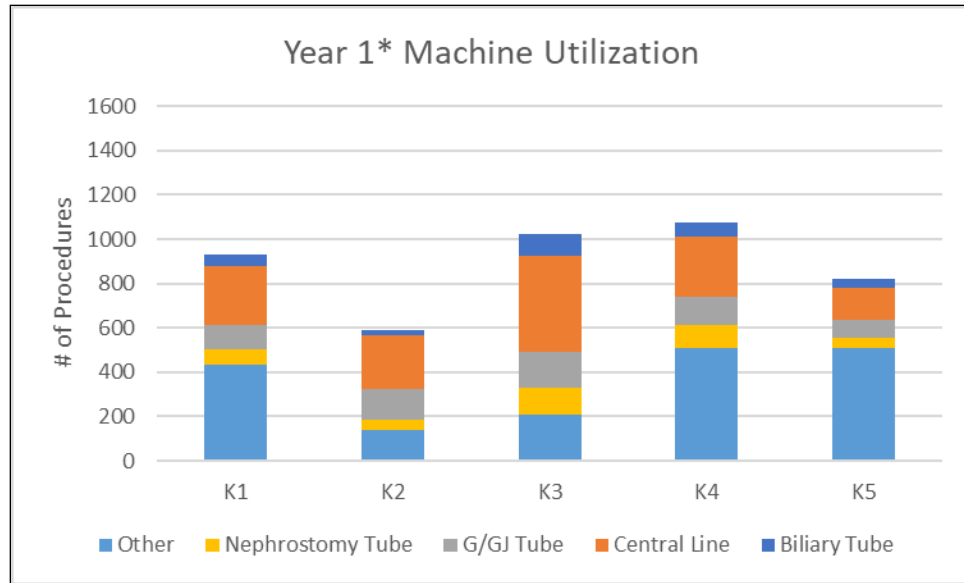


Figure 3.5: Yearly machine utilization for Jul 2019-Jun 2020. Data is incomplete for Oct 2019 due to technical issues which prevented procedure data from being transcribed to the RDSR.

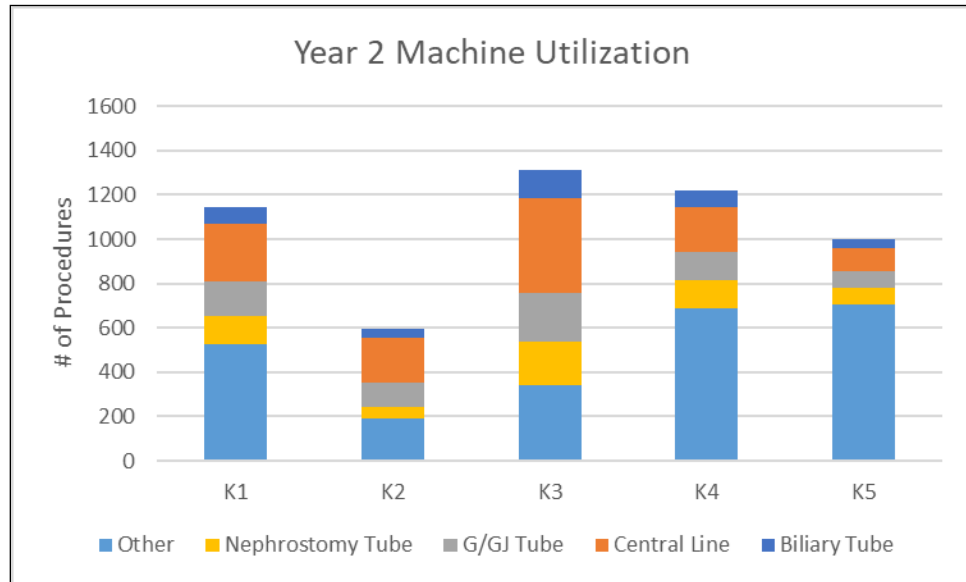


Figure 3.6: Yearly machine utilization for Jul 2020-Jun 2021

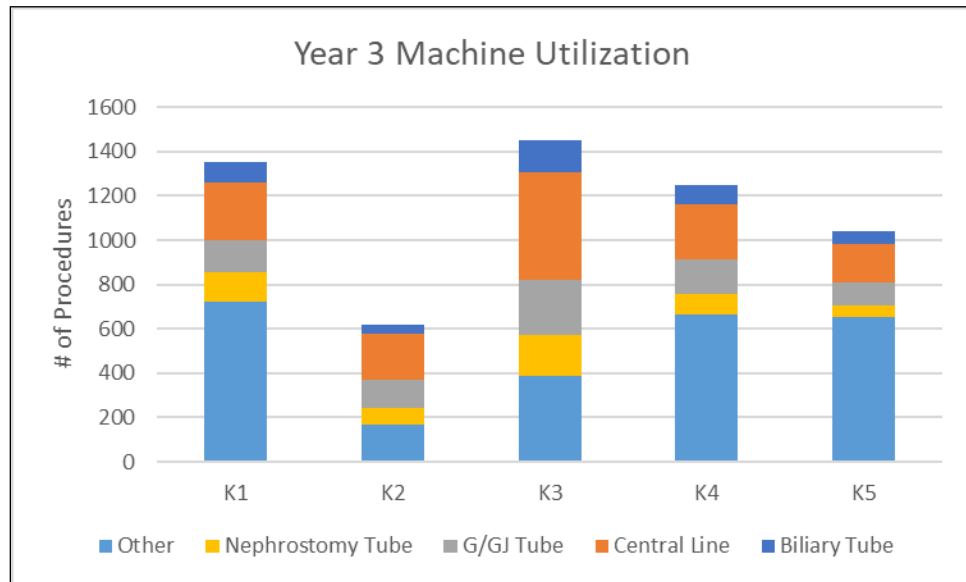


Figure 3.7: Yearly machine utilization for Aug 2021-Aug 2022

3.1.3 Discussion

This is a novel analysis framework with the specific aim of improving local dose reduction practices and subsequently lowering occupational exposures to a population of operators who typically receive high annual doses. This is a complicated problem not just because of the high degree of variability within each fluoroscopy procedure, but with a large group of operators performing large numbers of procedures there is also an aspect of workload/dose management among a group.

3.1.3.1 Machine Performance

AKRs from fluoscopy mode for each of the four procedure categories were compared across all IR units. In all four categories, K3 and K4 have a noticeably higher median AKR as well as larger variation in the AKRs between similar cases compared to the other units. The presence of this difference is not unexpected, but the magnitude was previously unknown and results from a combination of factors. Firstly, the three models being compared are known to have different filtration settings. When the low or medium fluoroscopy modes are selected, K1, K2, and K5 use .4 mm copper filtration compared to .1 mm copper used on K3 and K4. The additional filtration results in harder, more penetrating beams. With less photon penetration for the same kV settings, the AERCs on K3 and K4 need to make a larger adjustment to the mA to achieve the target image quality and results in higher AKRs than on K1, K2, and K5.

Another factor contributing to the differences in AK is the use of magnification. When considering the individual procedures, it is easy to assume that all else being equal, magnification would be used in similar proportions across the rooms. In surveying the operators, it was reported that magnification is used more frequently with K3 and K4 due to the display screens in those rooms being smaller than the screens in the other three rooms. Using magnification lowers the image quality by possible de-binning of detector elements and by magnifying the effects of quantum noise in the image. To counter these effects and maintain the target image quality the AERC will boost the SNR by increasing beam parameters such as mA and pulse width, leading to higher AKRs.

Although the AKR is noticeably higher on two of the IR units, a corresponding increase to operator dose can be mitigated by minimizing the field size through collimation and by utilizing the contour shields present in all rooms.

3.1.3.2 Machine Utilization

Figures 3.5 - 3.7 clearly demonstrate that K2 is utilized far less frequently by IR staff than any of the other units. This is because it is primarily used by the neurosurgery department whose procedures were outside the scope of this study. There was an increase in the total number of procedures performed year-to-year and the distribution of procedures among the five units is not equal throughout the three years.

As noted in Section 3.1.3.1, units K3 and K4 have much higher AKRs than the other three units.

3.2 Operator-Specific Differences

The following sections will attempt to address differences in procedure data unique to the individual operators. There are multiple clinical behaviors that can cause operators to receive different doses when performing the same procedure on the same machine. This section will investigate AKR, fluoroscopy time, and individual caseload indicators that can lead to occupational dose differences among staff.

As described in section 3.1, changes in AKR can lead to corresponding changes in occupational dose but are unable to be exactly quantified without direct measurement. When comparing AKR between similar procedures performed on the same unit, any resulting variation would be due to a combination of patient anatomy and selection of clinical settings. When performing procedures, operators can adjust between a low, medium, and high dose rate setting for normal fluoroscopy as well as a range of magnification sizes and SIDs, all of which would cause fluctuations in AK throughout the procedure. From a radiation protection standpoint, identifying large differences between operators and working to eliminate the variation in setting selections among operators will help to reduce the overall dose received by the group.

Dose from radiation exposure is proportional to the amount of time an individual is exposed. The two ways to reduce exposure time of operators that will be

addressed in this study are by reducing the amount of fluoroscopy time per procedure, and reducing the total number of procedures performed.

3.2.1 Materials and Methods

3.2.1.1 AKR Comparison

The columns from the data tables in Section 3.2.1.1 were subdivided to obtain tables representing the AKR of procedures done by individual operators on each unit. This data was analyzed using XLSTAT's Descriptive Statistics function. Operators with either a noticeably higher median or range compared to their peers for the same procedures on the same units were identified as potential targets for dose reduction strategies.

3.2.1.2 Fluoroscopy Time Comparison

For each provider, fluoroscopy times for Central Line procedures were separated by year and imported into MATLAB. In order to compare distributions of values, each dataset must be described by the same distribution function. Once the correct distribution is fit to the datasets, the relationships between datasets can be established by comparing the distribution parameters. Because fluoroscopy time per procedure can only be positive, is skewed to the right, and is concentrated close to its lower limit, the datasets meet the criteria for being described by a lognormal distribution [14].

A 10-bin histogram of each dataset was created and fit to a lognormal distribution. The fitted distributions for each provider were plotted together, and the distribution parameters for each were recorded.

3.2.1.3 Caseload Breakdown

For each year, the number of cases in each category performed by each operator was calculated and used to create Excel percentage stacked columns representing the proportional makeup of a provider's total caseload year-to-year. The total number of procedures as well as the breakdown of procedure types assigned to each provider year to year were evaluated. Operators whose overall caseload increased, or who had noticeable changes in the percentage of each procedure type that were assigned were noted as potential sources of increased occupational doses.

3.2.2 Results

3.2.2.1 AKR Comparison

Figures 3.8 through 3.27 show the spread of calculated air kerma rates for each provider broken down by unit and procedure type.

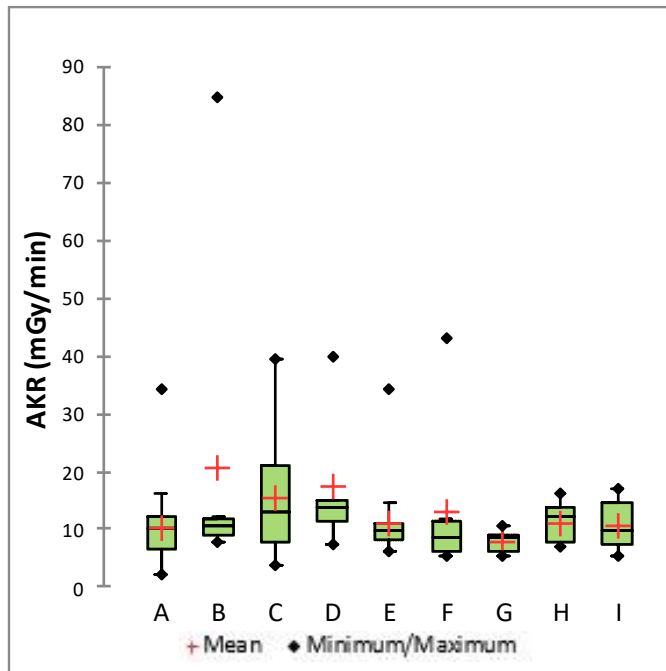


Figure 3.8: Comparison of operator AKRs for biliary tube procedures performed on K1 from Aug 2021-Aug 2022

Table 3.5: Numerical data for Figure 3.8

	A	B	C	D	E	F	G	H	I
Number of Procedures	17	7	10	5	16	7	10	7	13
AKR Statistic (mGy/min)									
Minimum	2.16	7.60	3.61	7.44	6.01	5.22	5.44	7.12	5.44
Maximum	34.18	84.85	39.33	40.01	34.34	42.92	10.66	16.24	16.95
1st Quartile	6.70	8.86	7.91	11.40	8.12	6.34	6.35	7.73	7.20
Median	10.35	10.43	12.90	13.91	9.71	8.52	8.40	12.07	9.76
3rd Quartile	12.23	11.90	21.10	14.99	11.07	11.38	9.05	13.67	14.52
Mean	10.38	20.63	15.45	17.55	10.97	13.16	7.94	11.17	10.67

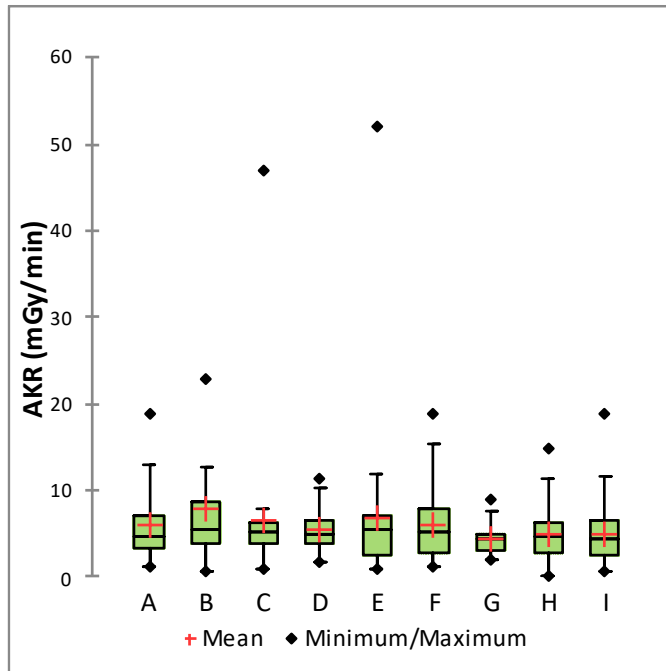


Figure 3.9: Comparison of operator AKRs for central line procedures performed on K1 from Aug 2021-Aug 2022

Table 3.6: Numerical data for Figure 3.9

	A	B	C	D	E	F	G	H	I
Number of Procedures	21	20	25	25	24	31	22	30	65
AKR Statistic (mGy/min)									
Minimum	1.27	0.60	0.85	1.67	1.00	1.24	1.90	0.20	0.77
Maximum	18.78	22.82	46.94	11.30	52.07	18.86	8.87	14.70	18.91
1st Quartile	3.26	3.87	3.78	3.91	2.63	2.76	2.94	2.82	2.44
Median	4.70	5.43	5.07	4.96	5.53	5.16	4.44	4.62	4.42
3rd Quartile	7.12	8.60	6.14	6.55	6.95	7.84	4.97	6.32	6.63
Mean	6.07	7.74	6.40	5.54	6.75	6.07	4.35	4.91	4.97

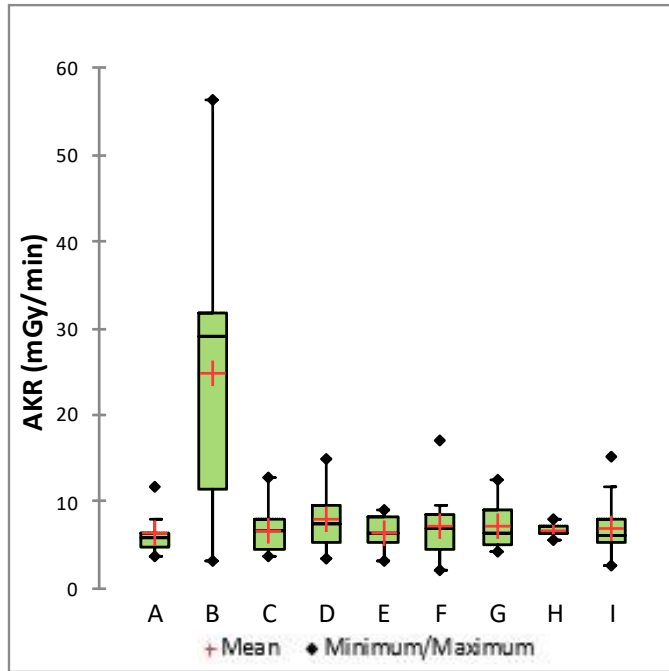


Figure 3.10: Comparison of operator AKRs for G/GJ tube procedures performed on K1 from Aug 2021-Aug 2022

Table 3.7: Numerical data for Figure 3.10

	A	B	C	D	E	F	G	H	I
Number of Procedures	10	9	10	14	14	11	8	5	60
AKR Statistic (mGy/min)									
Minimum	3.67	3.15	3.64	3.46	3.11	2.18	4.27	5.45	2.67
Maximum	11.67	56.26	12.79	14.93	8.90	17.06	12.59	7.96	15.28
1st Quartile	4.88	11.51	4.45	5.35	5.21	4.44	5.06	6.27	5.18
Median	5.78	29.02	6.61	7.35	6.26	6.98	6.30	6.44	6.20
3rd Quartile	6.40	31.80	7.89	9.56	8.31	8.52	9.03	7.28	7.97
Mean	6.23	24.87	6.70	7.98	6.36	7.13	7.20	6.68	6.86

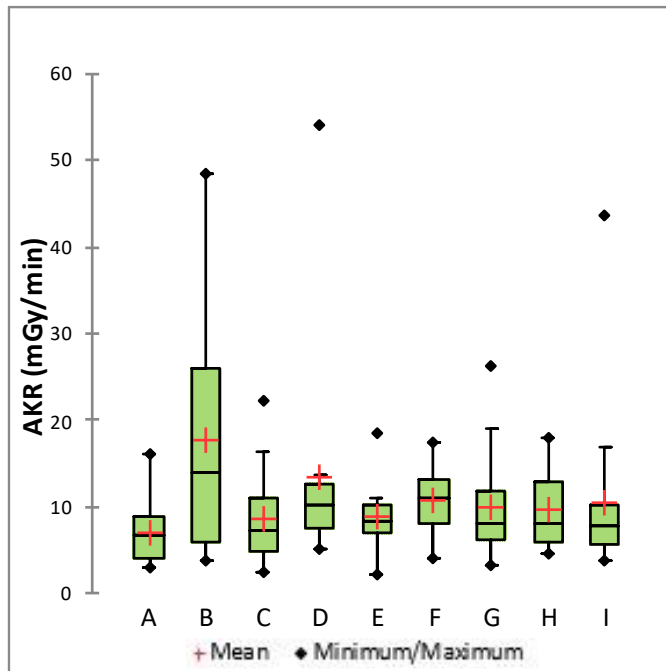


Figure 3.11: Comparison of operators AKRs for nephrostomy tube procedures performed on K1 from Aug 2021-Aug 2022

Table 3.8: Numerical data for Figure 3.11

	A	B	C	D	E	F	G	H	I
Number of Procedures	13	13	19	18	9	8	21	10	22
AKR Statistic (mGy/min)									
Minimum	2.90	3.86	2.35	5.23	2.18	3.91	3.31	4.46	3.66
Maximum	16.00	48.55	22.21	54.10	18.46	17.47	26.29	17.99	43.61
1st Quartile	4.00	6.00	4.71	7.41	6.93	8.09	6.06	5.90	5.62
Median	6.58	13.85	7.25	10.20	8.27	11.06	8.07	8.09	7.72
3rd Quartile	8.87	25.99	10.89	12.64	10.23	13.01	11.87	12.78	10.17
Mean	7.01	17.64	8.53	13.46	8.77	10.70	9.81	9.53	10.52

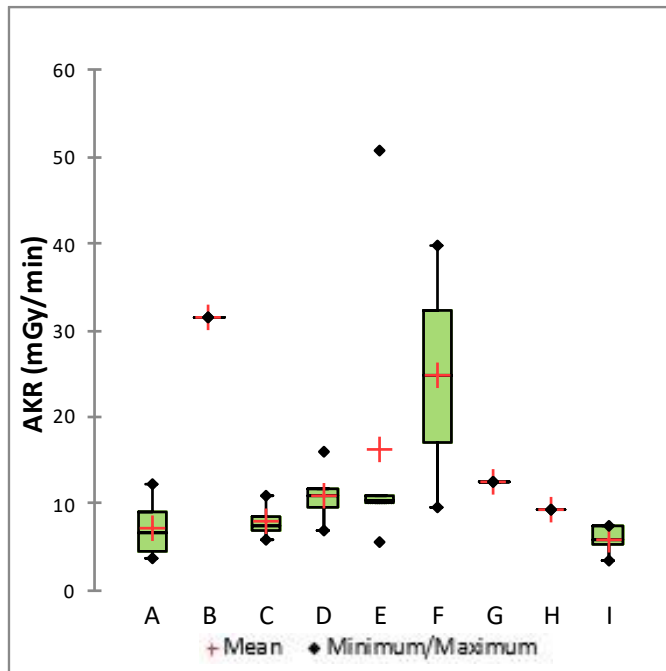


Figure 3.12: Comparison of operator AKRs for biliary tube procedures performed on K2 from Aug 2021-Aug 2022

Table 3.9: Numerical data for Figure 3.12

	A	B	C	D	E	F	G	H	I
Number of Procedures	12	1	4	5	6	2	1	1	5
AKR Statistic (mGy/min)									
Minimum	3.70	31.56	5.77	6.85	5.58	9.59	12.49	9.23	3.50
Maximum	12.21	31.56	10.83	16.02	50.87	39.87	12.49	9.23	7.43
1st Quartile	4.48	31.56	6.84	9.44	10.07	17.16	12.49	9.23	5.38
Median	6.55	31.56	7.48	11.03	10.24	24.73	12.49	9.23	5.85
3rd Quartile	9.07	31.56	8.52	11.70	10.78	32.30	12.49	9.23	7.38
Mean	7.06	31.56	7.89	11.01	16.32	24.73	12.49	9.23	5.91

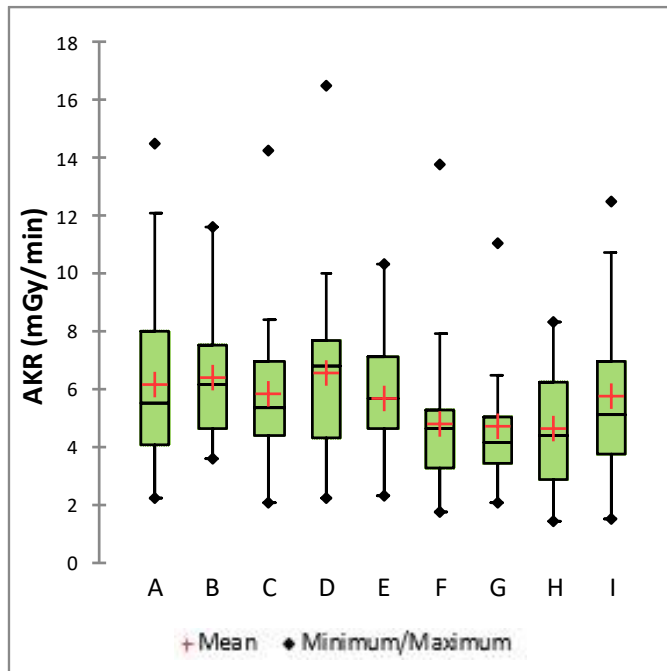


Figure 3.13: Comparison of operator AKRs for central line procedures performed on K2 from Aug 2021-Aug 2022

Table 3.10: Numerical data for Figure 3.13

	A	B	C	D	E	F	G	H	I
Number of Procedures	26	13	29	21	17	25	17	12	48
AKR Statistic (mGy/min)									
Minimum	2.23	3.59	2.03	2.22	2.33	1.74	2.07	1.44	1.50
Maximum	14.48	11.59	14.30	16.54	10.35	13.82	11.06	8.29	12.47
1st Quartile	4.06	4.67	4.40	4.29	4.60	3.25	3.46	2.90	3.77
Median	5.51	6.12	5.35	6.81	5.66	4.64	4.13	4.42	5.12
3rd Quartile	8.01	7.50	6.97	7.67	7.13	5.28	5.07	6.22	6.96
Mean	6.17	6.44	5.84	6.56	5.70	4.77	4.68	4.63	5.77

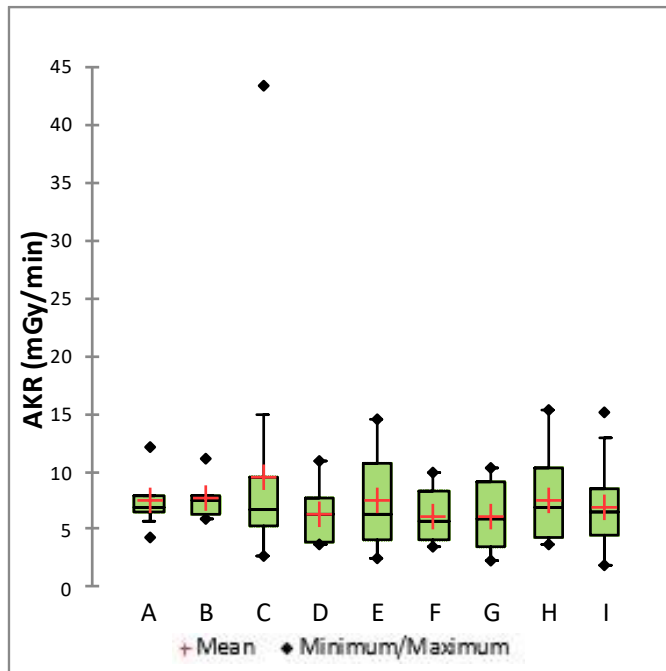


Figure 3.44: Comparison of operator AKRs for G/GJ tube procedures performed on K2 from Aug 2021-Aug 2022

Table 3.11: Numerical data for Figure 3.14

	A	B	C	D	E	F	G	H	I
Number of Procedures	13	5	14	8	9	10	8	9	50
AKR Statistic (mGy/min)									
Minimum	4.37	5.85	2.77	3.64	2.41	3.50	2.25	3.66	1.92
Maximum	12.03	11.21	43.43	10.94	14.63	9.98	10.34	15.42	15.04
1st Quartile	6.57	6.27	5.24	3.94	4.14	4.10	3.52	4.20	4.56
Median	6.81	7.54	6.75	6.33	6.37	5.74	5.90	6.84	6.51
3rd Quartile	7.86	7.83	9.47	7.65	10.65	8.21	9.07	10.27	8.56
Mean	7.58	7.74	9.61	6.33	7.46	6.18	6.20	7.55	6.83

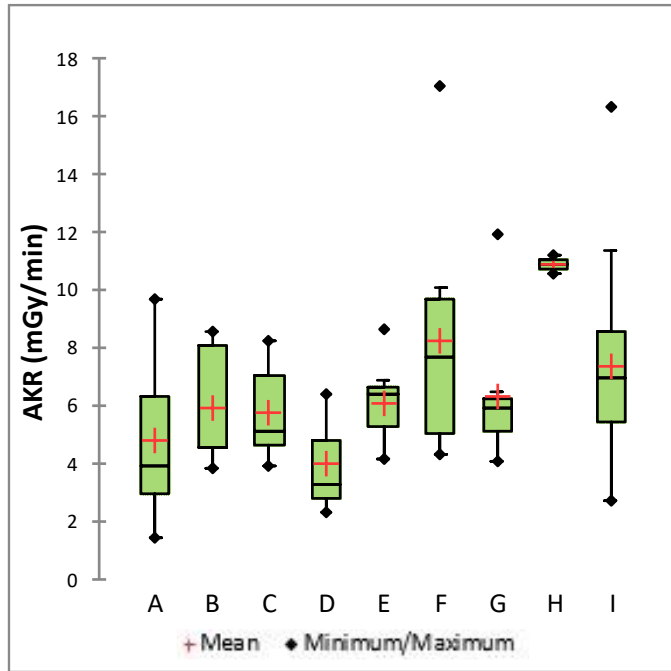


Figure 3.55: Comparison of operator AKRs for nephrostomy tube procedures performed on K2 from Aug 2021-Aug 2022

Table 3.12: Numerical data for Figure 3.15

	A	B	C	D	E	F	G	H	I
Number of Procedures	6	5	10	3	8	9	8	2	28
AKR Statistic (mGy/min)									
Minimum	1.40	3.84	3.93	2.30	4.16	4.29	4.08	10.59	2.72
Maximum	9.65	8.58	8.26	6.39	8.67	17.09	11.91	11.23	16.33
1st Quartile	2.95	4.52	4.64	2.78	5.28	5.07	5.11	10.75	5.48
Median	3.89	4.56	5.15	3.26	6.38	7.70	5.91	10.91	6.97
3rd Quartile	6.30	8.08	7.05	4.83	6.63	9.69	6.22	11.07	8.53
Mean	4.76	5.92	5.79	3.98	6.11	8.25	6.31	10.91	7.34

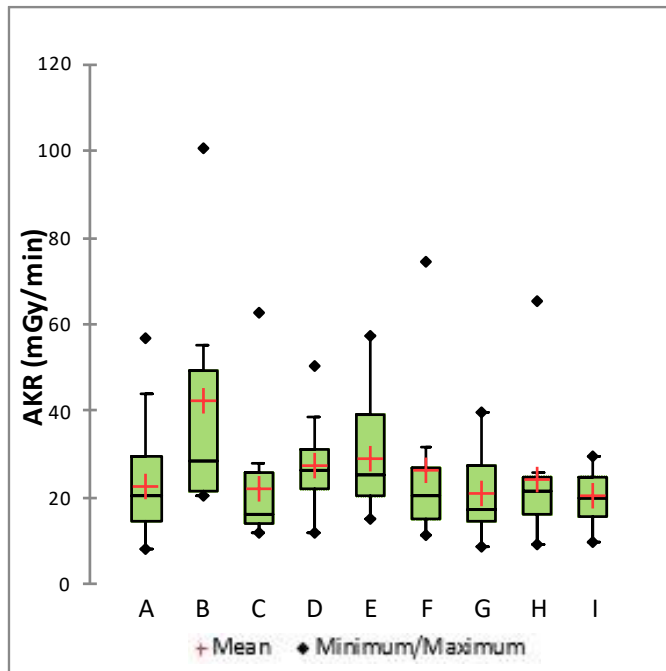


Figure 3.66: Comparison of operator AKRs for biliary tube procedures performed on K3 from Aug 2021-Aug 2022

Table 3.13: Numerical data for Figure 3.16

	A	B	C	D	E	F	G	H	I
Number of Procedures	32	6	13	10	24	16	15	14	18
AKR Statistic (mGy/min)									
Minimum	7.96	20.41	11.74	12.07	15.21	11.07	8.65	8.91	9.42
Maximum	56.94	100.81	62.52	50.08	57.34	74.35	39.71	65.42	29.26
1st Quartile	14.47	21.31	13.74	22.09	20.44	15.27	14.29	15.95	15.61
Median	20.44	28.24	16.35	26.40	25.15	20.34	17.09	21.64	19.76
3rd Quartile	29.61	49.36	25.61	30.82	39.08	26.93	27.51	24.77	24.92
Mean	22.49	42.18	21.83	27.21	29.06	26.44	20.94	24.27	20.56

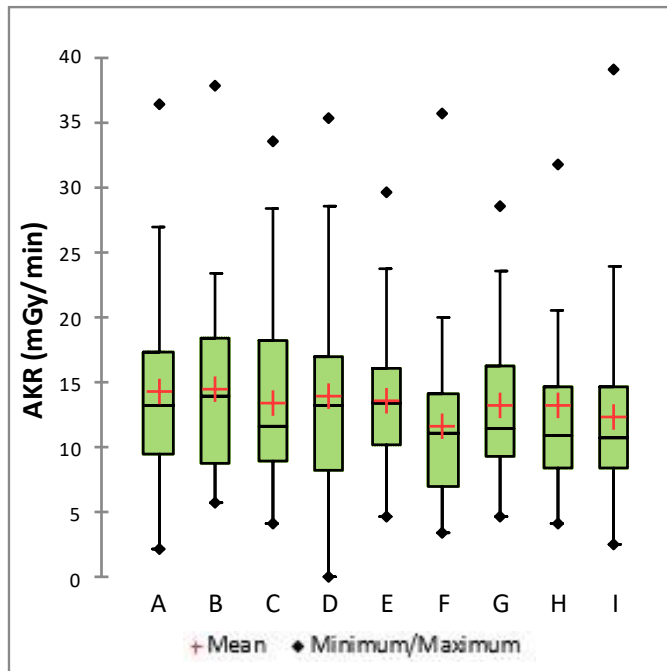


Figure 3.77: Comparison of operators AKRs for central line tube procedures performed on K3 from Aug 2021-Aug 2022

Table 3.14: Numerical data for Figure 3.17

	A	B	C	D	E	F	G	H	I
Number of Procedures	47	37	65	59	40	73	44	32	86
AKR Statistic (mGy/min)									
Minimum	2.194	5.70	4.25	0.00	4.67	3.54	4.64	4.13	2.53
Maximum	36.49	37.94	33.68	35.43	29.63	35.80	28.58	31.89	39.16
1st Quartile	9.58	8.84	9.04	8.29	10.26	6.98	9.27	8.53	8.42
Median	13.29	14.04	11.71	13.20	13.42	11.14	11.49	10.94	10.85
3rd Quartile	17.38	18.49	18.19	17.10	16.20	14.14	16.39	14.70	14.67
Mean	14.36	14.48	13.50	13.91	13.62	11.69	13.33	13.18	12.40

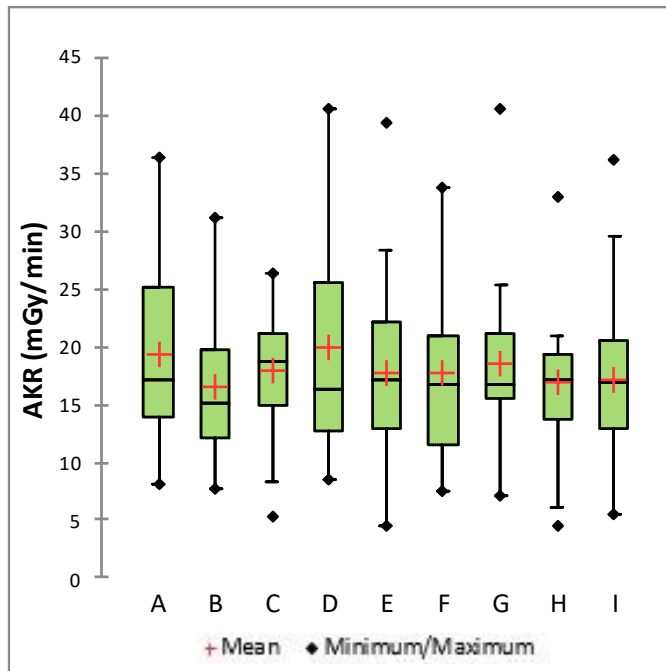


Figure 3.18: Comparison of operator AKRs for G/GJ tube procedures performed on K3 from Aug 2021-Aug 2022

Table 3.15: Numerical data for Figure 3.18

	A	B	C	D	E	F	G	H	I
Number of Procedures	16	11	25	22	31	25	28	18	71
AKR Statistic (mGy/min)									
Minimum	8.11	7.72	5.27	8.45	4.55	7.54	7.18	4.59	5.53
Maximum	36.40	31.14	26.38	40.60	39.47	33.69	40.68	33.03	36.17
1st Quartile	13.99	12.03	14.97	12.67	12.83	11.45	15.44	13.79	12.88
Median	17.10	15.19	18.84	16.33	17.14	16.81	16.66	17.05	17.02
3rd Quartile	25.26	19.67	21.18	25.51	22.12	21.00	21.22	19.35	20.45
Mean	19.42	16.56	17.97	19.97	17.74	17.74	18.62	16.94	17.16

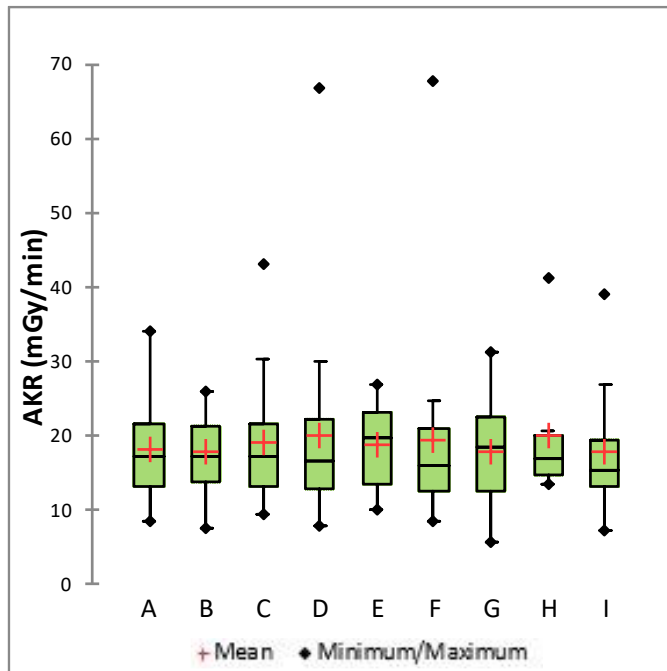


Figure 3.198: Comparison of operator AKRs for nephrostomy tube procedures performed on K3 from Aug 2021-Aug 2022

Table 3.16: Numerical data for Figure 3.19

	A	B	C	D	E	F	G	H	I
Number of Procedures	29	14	22	19	10	32	14	10	40
AKR Statistic (mGy/min)									
Minimum	8.33	7.39	9.41	7.92	9.95	8.31	5.63	13.58	7.18
Maximum	34.03	26.05	42.95	66.86	27.02	67.79	31.39	41.34	39.15
1st Quartile	13.02	13.81	13.26	12.80	13.33	12.55	12.57	14.74	13.15
Median	17.14	17.05	17.30	16.58	19.81	15.84	18.40	16.97	15.47
3rd Quartile	21.58	21.29	21.47	22.16	23.10	20.97	22.56	19.92	19.27
Mean	18.12	17.67	19.10	19.90	18.83	19.44	17.90	19.96	17.68

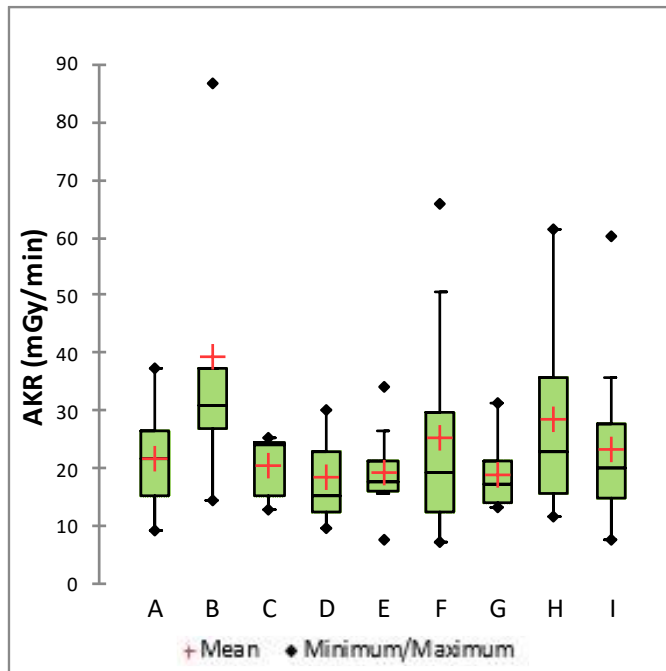


Figure 3.90: Comparison of operator AKRs for biliary tube procedures performed on K4 from Aug 2021-Aug 2022

Table 3.17: Numerical data for Figure 3.20

	A	B	C	D	E	F	G	H	I
Number of Procedures	19	5	5	3	10	11	7	10	14
AKR Statistic (mGy/min)									
Minimum	9.35	14.33	12.85	9.86	7.77	7.17	13.24	11.80	7.85
Maximum	37.18	86.58	25.22	29.97	33.96	66.02	31.26	61.45	60.37
1st Quartile	15.33	26.89	15.44	12.66	16.18	12.48	14.15	15.49	14.98
Median	21.73	31.02	24.18	15.47	17.74	19.11	17.47	22.94	20.14
3rd Quartile	26.34	37.15	24.36	22.72	21.45	29.70	21.32	35.66	27.62
Mean	21.57	39.19	20.41	18.43	19.34	25.42	18.99	28.59	23.27

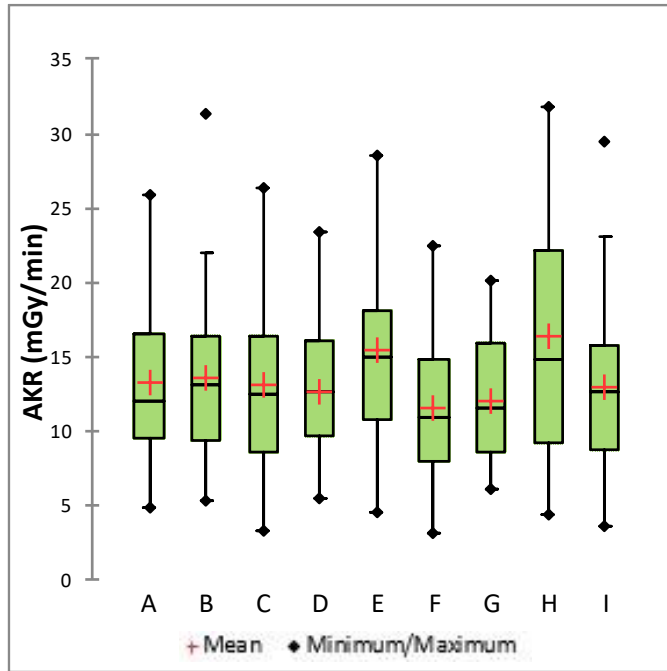


Figure 3.101: Comparison of operator AKRs for central line procedures performed on K4 from Aug 2021-Aug 2022

Table 3.18: Numerical data for Figure 3.21

	A	B	C	D	E	F	G	H	I
Number of Procedures	36	28	22	23	17	29	18	17	58
AKR Statistic (mGy/min)									
Minimum	4.78	5.25	3.25	5.37	4.47	3.13	5.98	4.33	3.62
Maximum	25.90	31.38	26.40	23.40	28.48	22.48	20.08	31.82	29.48
1st Quartile	9.46	9.34	8.59	9.62	10.73	7.88	8.57	9.18	8.72
Median	12.03	13.04	12.49	12.57	15.00	10.84	11.53	14.72	12.61
3rd Quartile	16.47	16.34	16.34	16.08	18.12	14.77	15.83	22.15	15.68
Mean	13.17	13.53	13.03	12.64	15.38	11.56	11.98	16.41	12.84

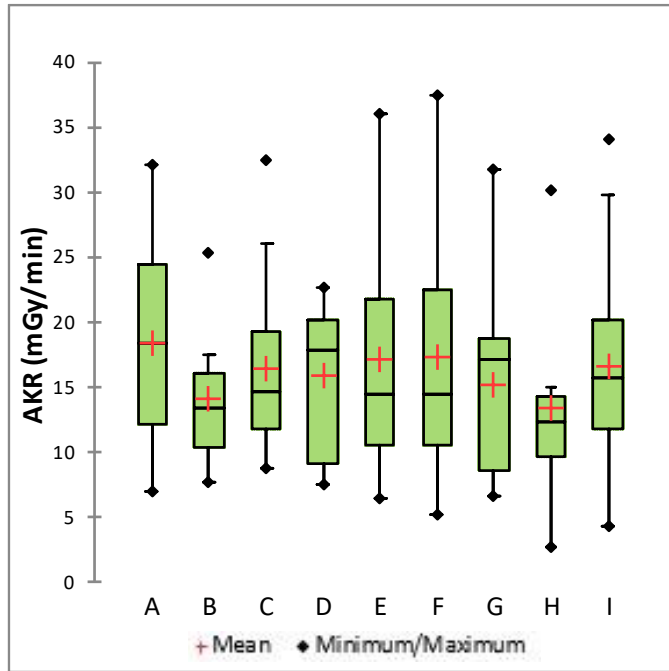


Figure 3.22: Comparison of operator AKRs for G/GJ tube procedures performed on K4 from Aug 2021-Aug 2022

Table 3.19: Numerical data for Figure 3.22

	A	B	C	D	E	F	G	H	I
Number of Procedures	20	8	23	12	22	16	13	11	32
AKR Statistic (mGy/min)									
Minimum	6.90	7.65	8.69	7.55	6.36	5.16	6.65	2.70	4.23
Maximum	32.20	25.37	32.47	22.63	35.96	37.44	31.79	30.14	34.12
1st Quartile	12.20	10.38	11.84	9.16	10.61	10.52	8.52	9.66	11.70
Median	18.31	13.36	14.69	17.93	14.52	14.42	17.13	12.31	15.73
3rd Quartile	24.51	16.03	19.19	20.22	21.84	22.53	18.66	14.37	20.13
Mean	18.35	14.17	16.44	15.89	17.09	17.36	15.16	13.32	16.53

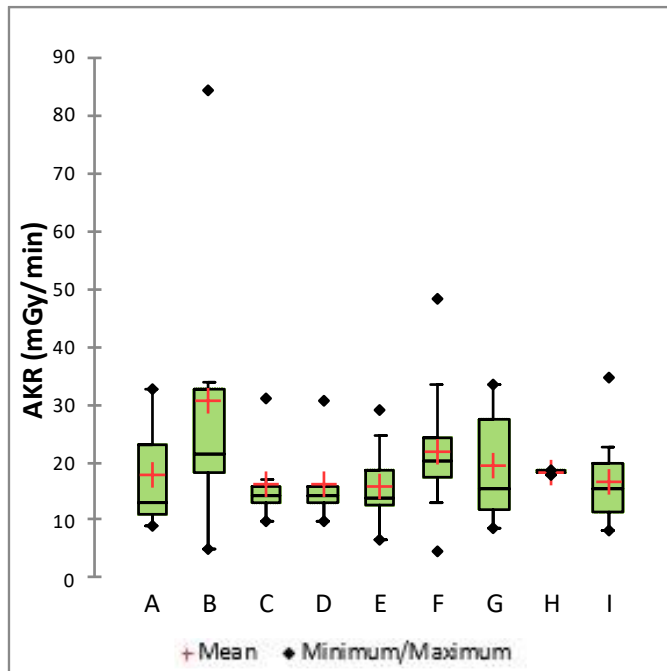


Figure 3.113: Comparison of AKRs for nephrostomy tube procedures performed by operators on K4 from Aug 2021-Aug 2022

Table 3.20: Numerical data for Figure 3.23

	A	B	C	D	E	F	G	H	I
Number of Procedures	9	10	7	6	12	18	8	2	20
AKR Statistic (mGy/min)									
Minimum	8.87	4.94	9.63	9.99	6.64	4.60	8.49	17.89	8.32
Maximum	32.85	84.60	31.00	30.75	29.23	48.42	33.57	18.79	34.82
1st Quartile	10.87	18.02	13.17	12.90	12.48	17.43	11.72	18.11	11.54
Median	12.98	21.53	14.03	14.10	14.00	20.14	15.54	18.34	15.25
3rd Quartile	23.13	32.73	15.64	15.67	18.64	24.26	27.49	18.56	19.64
Mean	17.64	30.49	16.04	16.27	15.75	21.88	19.38	18.34	16.81

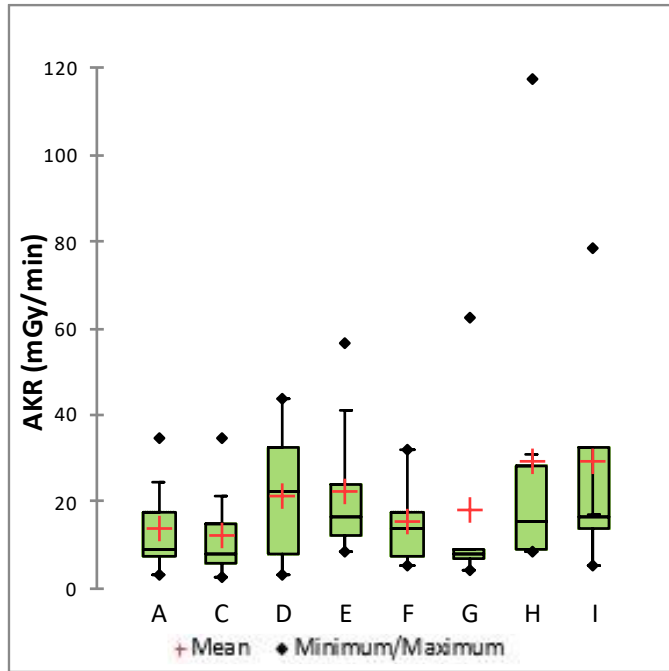


Figure 3.124: Comparison of operator AKRs for biliary tube procedures performed on K5 from Aug 2021-Aug 2022

Table 3.21: Numerical data for Figure 3.24

	A	C	D	E	F	G	H	I
Number of Procedures	13	7	7	9	5	5	10	4
AKR Statistic (mGy/min)								
Minimum	3.09	2.60	3.32	8.28	5.41	3.94	8.36	5.44
Maximum	34.81	34.75	43.90	56.67	31.95	62.56	117.33	78.62
1st Quartile	7.34	5.57	7.90	12.21	7.54	6.92	8.99	13.73
Median	8.78	7.81	22.07	16.28	13.75	7.63	15.27	16.68
3rd Quartile	17.27	14.80	32.48	23.90	17.35	9.08	28.18	32.31
Mean	13.83	12.27	21.43	22.43	15.20	18.03	29.49	29.36

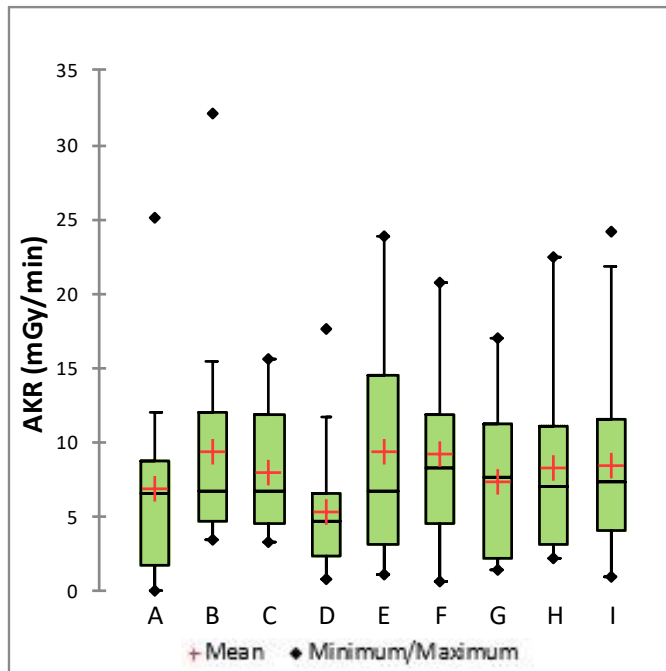


Figure 3.135: Comparison of operator AKRs for central line procedures performed on K5 from Aug 2021-Aug 2022

Table 3.22: Numerical data for Figure 3.25

	A	B	C	D	E	F	G	H	I
Number of Procedures	19	14	25	24	21	10	14	22	25
AKR Statistic (mGy/min)									
Minimum	0.00	3.42	3.21	0.73	1.09	0.58	1.30	2.09	0.97
Maximum	25.13	32.04	15.61	17.67	23.79	20.64	16.99	22.46	24.16
1st Quartile	1.67	4.62	4.47	2.37	3.07	4.42	2.08	3.04	3.98
Median	6.45	6.66	6.63	4.64	6.67	8.23	7.63	6.97	7.25
3rd Quartile	8.63	11.91	11.89	6.59	14.52	11.86	11.18	11.06	11.55
Mean	6.88	9.35	7.87	5.25	9.29	9.22	7.34	8.22	8.46

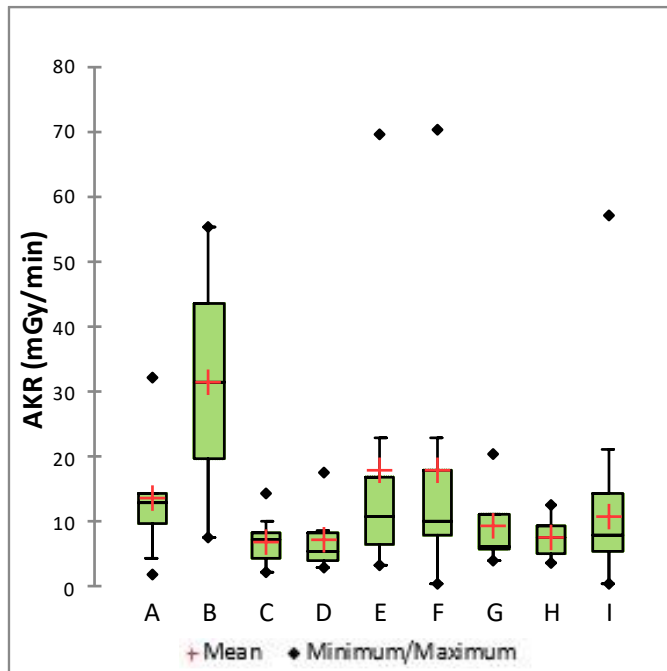


Figure 3.146: Comparison of operator AKRs for G/GJ tube procedures performed on K5 from Aug 2021-Aug 2022

Table 3.23: Numerical data for Figure 3.26

	A	B	C	D	E	F	G	H	I
Number of Procedures	10	2	11	13	8	13	5	10	29
AKR Statistic (mGy/min)									
Minimum	1.93	7.79	2.46	2.99	3.29	0.63	3.91	3.83	0.39
Maximum	32.23	55.51	14.49	17.54	69.58	70.39	20.31	12.65	57.33
1st Quartile	9.91	19.72	4.56	3.96	6.67	7.98	5.93	4.98	5.51
Median	12.88	31.65	7.43	5.67	10.84	10.17	6.36	7.46	7.82
3rd Quartile	14.35	43.58	8.40	8.25	16.77	17.97	11.04	9.35	14.31
Mean	13.68	31.65	7.04	7.20	18.07	17.82	9.51	7.63	10.89

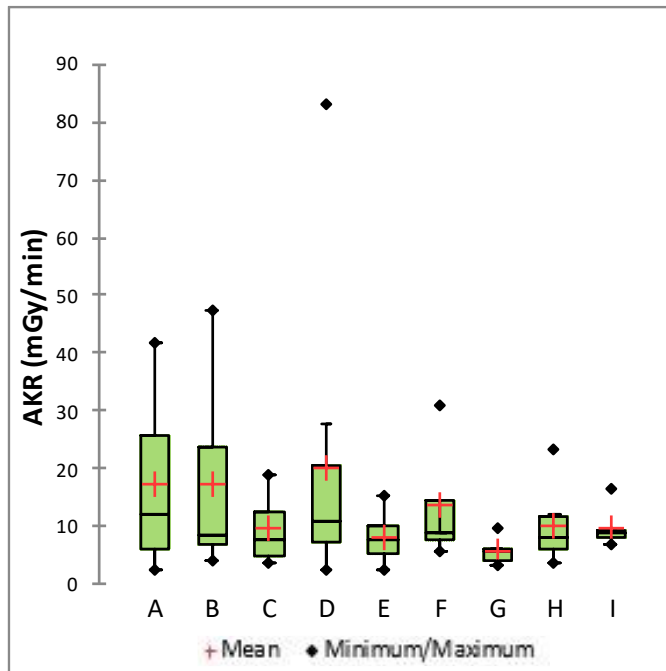


Figure 3.157: Comparison of operator AKRs for nephrostomy tube procedures performed on K5 from Aug 2021-Aug 202

Table 3.24: Numerical data for Figure 3.27

	A	B	C	D	E	F	G	H	I
Number of Procedures	6	6	4	9	6	4	6	6	7
AKR Statistic (mGy/min)									
Minimum	2.27	4.23	3.69	2.27	2.50	5.68	3.15	3.81	6.93
Maximum	41.94	47.20	18.92	83.23	15.15	31.11	9.54	23.18	16.60
1st Quartile	6.00	6.99	4.64	7.05	5.21	7.74	3.98	6.12	7.93
Median	12.14	8.37	7.73	10.83	7.73	8.71	5.78	8.17	8.96
3rd Quartile	25.90	23.82	12.61	20.37	9.87	14.53	6.15	11.62	9.19
Mean	17.15	17.28	9.52	20.12	8.01	13.55	5.65	10.26	9.53

3.2.2.2 Fluoroscopy Time Comparison

Figures 3.28 through 3.37 show the lognormal distribution fits of the fluoroscopy time for central line procedures performed by each provider between Jul 2019 and Aug 2022. The distribution parameters for each dataset are listed in table 3.25.

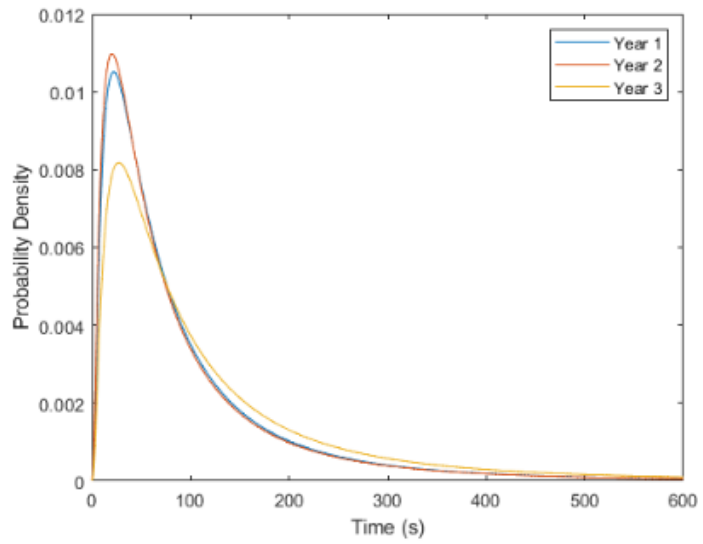


Figure 3.168: Lognormal fit of fluoroscopy times for central line procedures performed by provider A over a three-year period.

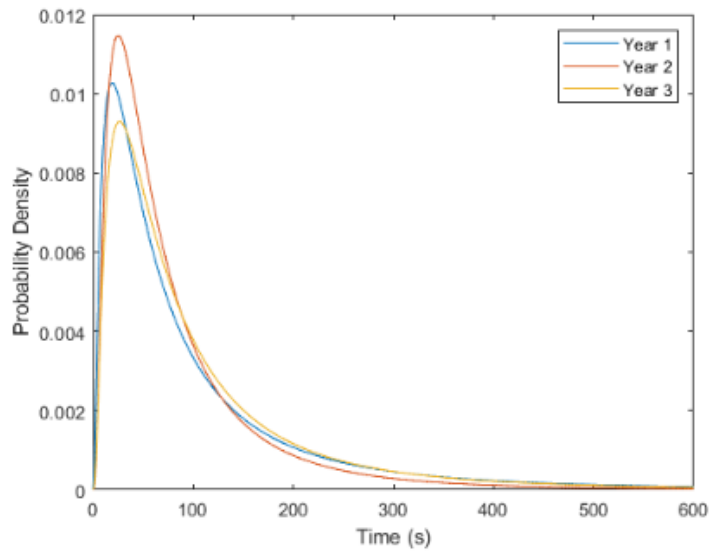


Figure 3.29: Lognormal fit of fluoroscopy times for central line procedures performed by provider B over a three-year period.

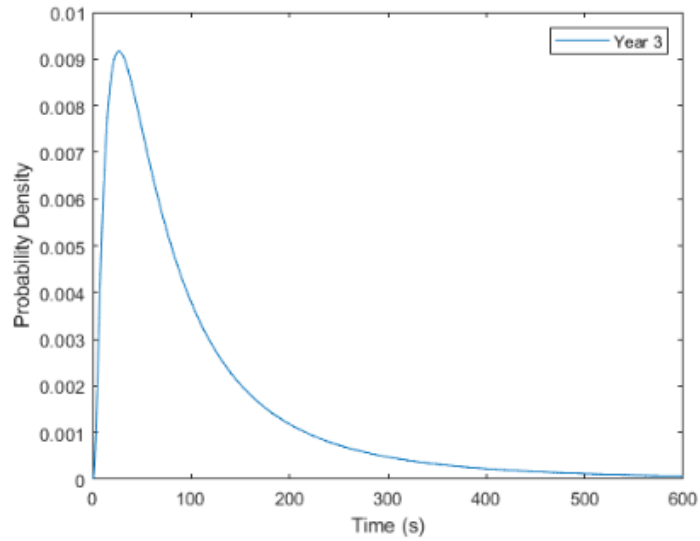


Figure 3.170: Lognormal fit of fluoroscopy times for central line procedures performed by provider C over a one-year period.

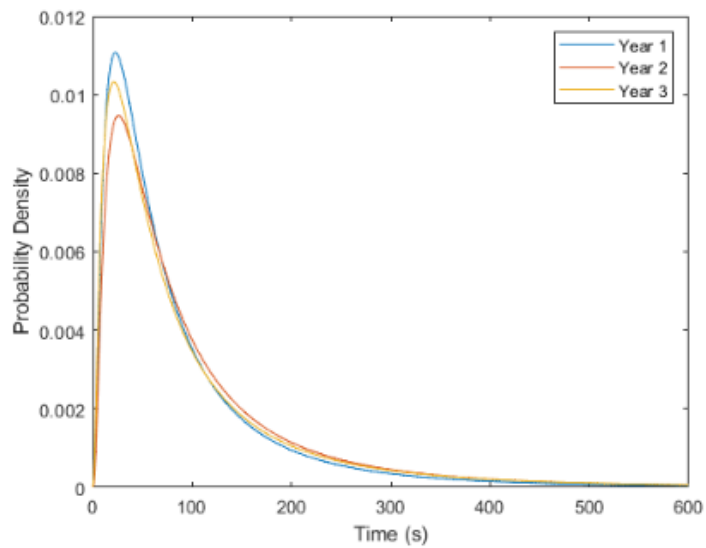


Figure 3.181: Lognormal fit of fluoroscopy times for central line procedures performed by provider D over a three-year period.

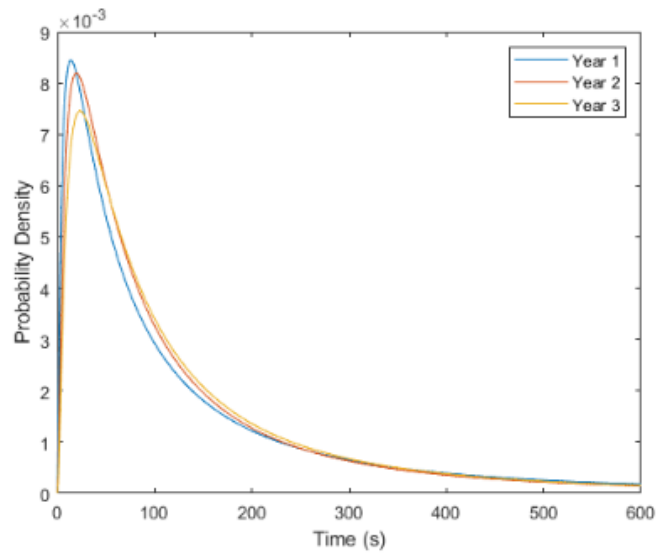


Figure 3.192: Lognormal fit of fluoroscopy times for central line procedures performed by provider E over a three-year period.

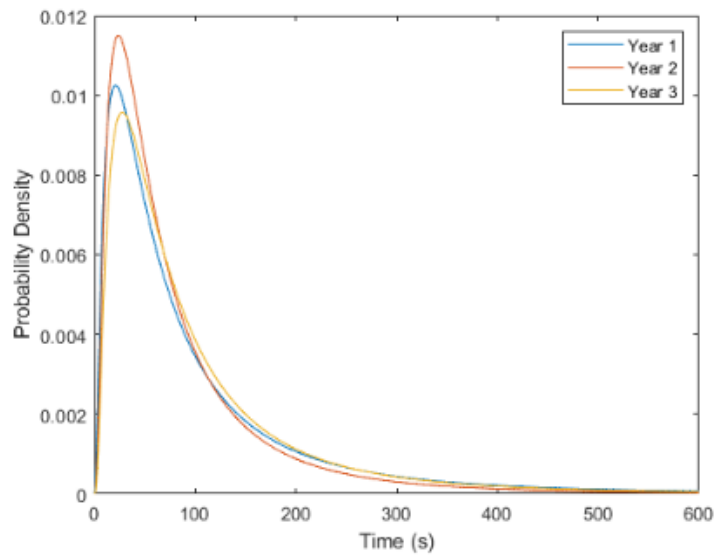


Figure 3.203: Lognormal fit of fluoroscopy times for central line procedures performed by provider F over a three-year period.

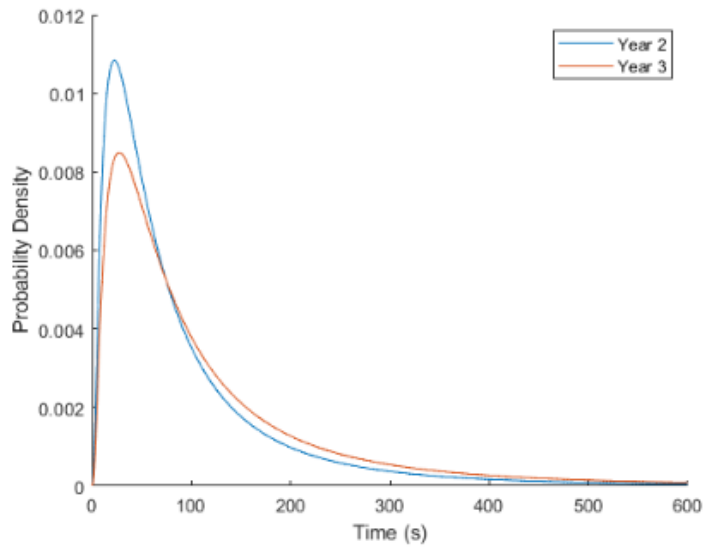


Figure 3.214: Lognormal fit of fluoroscopy times for central line procedures performed by provider G over a two-year period.

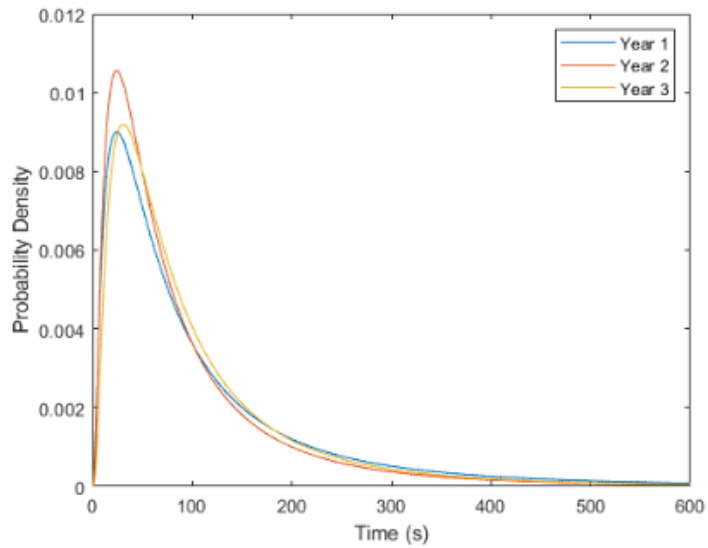


Figure 3.225: Lognormal fit of fluoroscopy times for central line procedures performed by provider H over a three-year period.

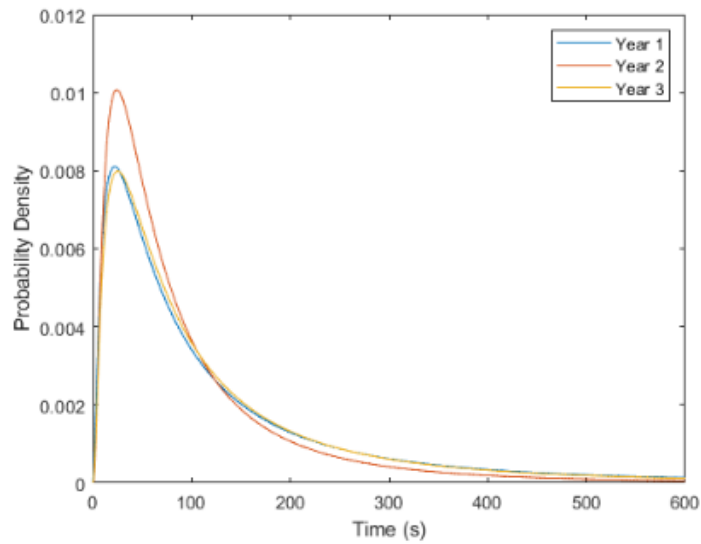


Figure 3.236: Lognormal fit of fluoroscopy times for central line procedures performed by provider I over a three-year period.

Table 3.25: Distribution parameters for the lognormal fits plotted in Figures 3.28 through 3.36

	μ			σ		
	Year 1	Year 2	Year 3	Year 1	Year 2	Year 3
A	4.137	4.094	4.389	1.026	1.044	1.044
B	4.170	4.056	4.259	1.106	0.9131	0.991
C	-	-	4.270	-	-	0.994
D	4.085	4.241	4.157	0.982	0.992	1.052
E	4.471	4.426	4.507	1.359	1.207	1.168
F	4.164	4.051	4.232	1.059	0.939	0.956
G	-	4.106	4.350	-	0.998	1.019
H	4.294	4.133	4.276	1.051	0.974	0.922
I	4.419	4.179	4.420	1.153	0.996	1.096

3.2.2.3 Caseload Breakdown

The figures below show the caseload breakdown of each provider from July 2019 – August 2022. In Year 1 and Year 2, the departmental caseload is divided between eight operators. In Year 3, the departmental caseload is split between nine operators. Despite adding an additional staff member in Year 3, Operators A, B, D, E, and F maintain a similar number of procedures while Provider I's caseload had a slight increase. The only personnel whose caseload decreased were Operators G and H.

Throughout the three years, most operators show an increase in the number of cases performed, even when using the monthly average number of procedures to estimate the missing data in October 2019. Provider I not only performed a consistently higher number of procedures than the others, but the disparity between Provider I and the remaining staff increases each year. At the same time, Provider H shows a notable decrease from year to year.

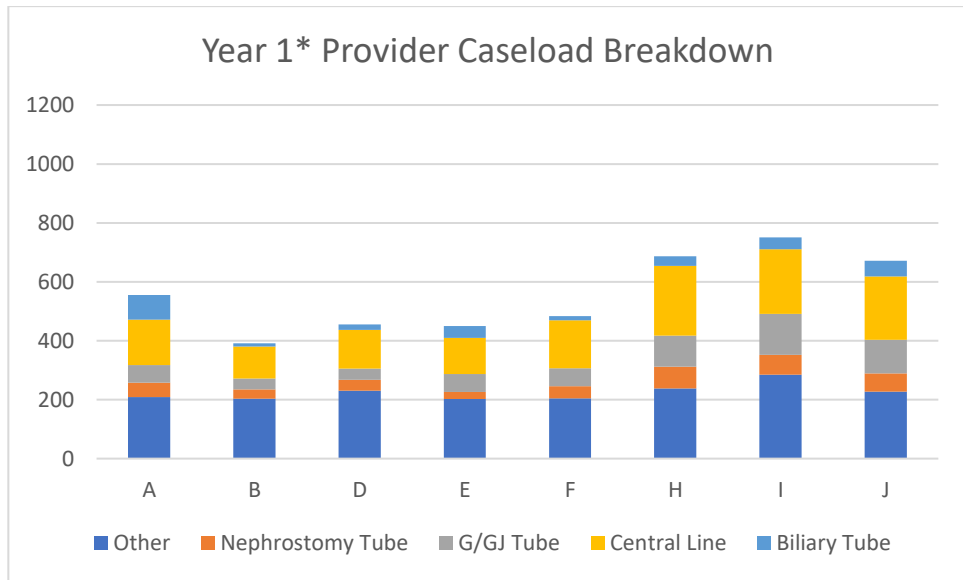


Figure 3.37: Yearly provider caseload breakdown for Jul 2019-Jun 2020. Data is incomplete for Oct 2019 due to network issues which prevented procedure information from being transcribed to the RDSR.

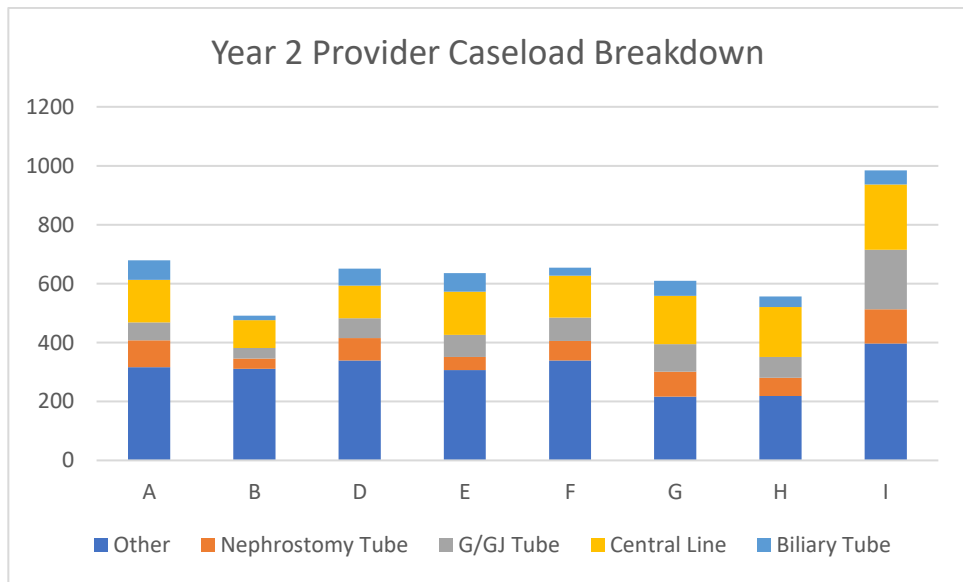


Figure 3.38: Yearly provider caseload breakdown for Jul 2020-Jun 2021

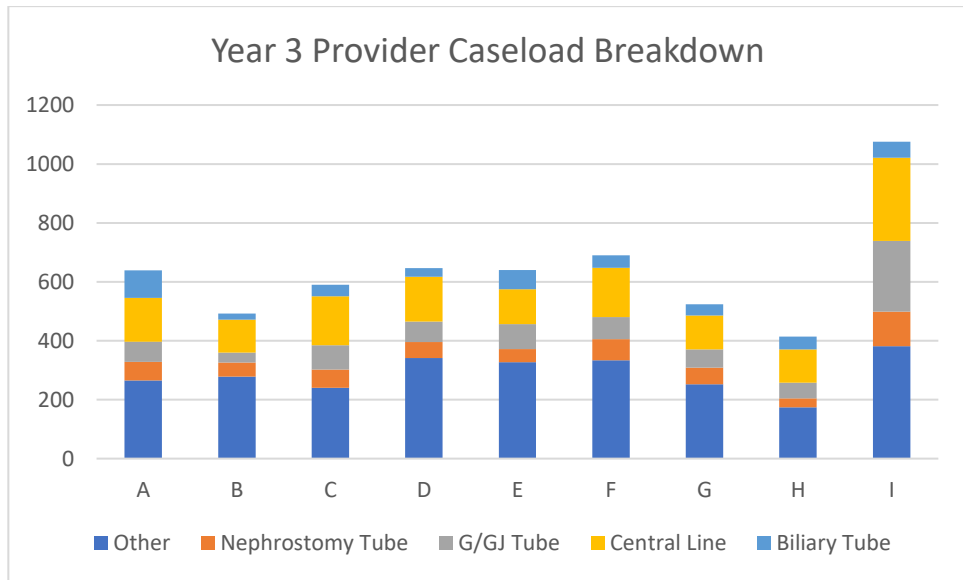


Figure 3.24: Yearly provider caseload breakdown for Aug 2021-Aug 2022

3.2.3 Discussion

3.2.3.1 AKR Comparison

AKR is a measure of the overall intensity of the primary beam. As demonstrated in Figures 3.1 through 3.4, the recorded AKR for similar procedures fluctuates between machines, with K3 and K4 generally having higher outputs than the other units. These graphs were generated using a large number of procedures performed by nine different personnel, and as noted in Chapter 2, there are clinical settings that can be adjusted by the operators which also have an effect on air kerma.

The data used to generate Figures 3.1 through 3.4 was further subdivided to be able to compare the operators. It is assumed that for each unit, the AERC response

would be consistent under the same protocol selections and the same procedures, with variability in the AKR resulting from differences in patient thickness and the fluoroscopy modes chosen by the operator. In this case, there is also variability introduced from grouping multiple procedures into categories, but this is limited due to the high level of similarity between the procedures in each category.

In looking at the AKRs of individual operators, a low median value is interpreted to demonstrate effective use of low-dose techniques during procedures, and a low spread of values is interpreted to indicate consistency in the fluoroscopy settings used from procedure to procedure. Operators with higher median AKR values and/or a larger spread of values should be identified for further evaluation of their utilization of dose reduction techniques.

3.2.3.2 Fluoroscopy Time Comparison

In statistics, μ is commonly used to denote the mean value of a population. This is not true in the case of a lognormal distribution. The median of a lognormal distribution is e^μ . A direct comparison of μ allows for qualitative identification of trends in the median fluoroscopy time used by each provider, and quantification of these trends would require comparing e^μ values.

Operators identified as having consistently higher median fluoroscopy times should be identified for further evaluation of clinical practices since higher fluoroscopy

times contribute to increased occupational dose. An operator's median fluoroscopy times can also be compared to their own historical data. Noticeable increases in fluoroscopy time for the same procedures over a period of time can indicate 1) that the operator is given more challenging cases than others, 2) that the operator is spending more time training new operators, or 3) that the operator in question has lost some amount of proficiency in the procedure or with the imaging system. Depending on the reason for the increase, this could be mitigated by instituting proficiency requirements to ensure a minimum number of procedures assigned to each operator and trainee to maintain proficiency. In situations where there are not enough actual cases to perform this minimum, other forms of training such as observation or skills can be substituted. Similarly, decreasing median fluoroscopy times can indicate 1) an operator is no longer training others, 2) an operator has gained proficiency over time, or 3) there has been a change in clinical practice that is more efficient than previous techniques.

In cases where operators are providing training to residents, it is impossible to determine based solely on the RDSR data whether the operator is performing the procedure, or whether the trainee is performing the procedure under supervision. The only way to correctly attribute procedure data to a trainee is to directly observe and annotate which procedures the trainee performed. For this study, no direct observations

were available for the historical data used, and all procedures were attributed to the attending who was listed on the RDSR regardless of whether a trainee was listed.

3.2.3.3 Caseload Breakdown

The number of cases an operator performs has a direct effect on occupational dose because it necessarily increases the cumulative exposure from fluoroscopy over a period of time. The amount of fluoroscopy utilized between different procedure types can vary greatly, so the distribution of types of cases assigned to a provider should be considered in addition to the overall number of procedures.

The four procedure categories identified in this study consist of procedures that occur very frequently but do not contribute very significantly to operator dose based on the cumulative (DAP). There are over 50 procedure types included in the “Other” category, many of which involve using a significant amount of fluoroscopy or cine and can also involve a range of frame rates compared to those used in the procedure categories assessed in this study. If an individual is noted to have an increase in occupational dose and their practices are determined to appropriately employ dose reduction methods, the next step is to look at their caseload. Two changes that could be the cause of increased dose to the operator are: a significant increase in the total number of procedures, and/or an increase in the percentage of high-dose procedures that are assigned to the operator.

Assessing the caseload breakdown of operators can also be beneficial in cases where dosimetry records are inconsistent. Assuming that clinical techniques are similar between operators, two individuals who have similar caseloads can be reasonably expected to have similar dosimetry readings. This relationship can be useful for occupational dosimetry program managers which need a way to predict whether personnel are approaching their exposure limit if they either do not consistently wear the assigned occupational dosimeter or do not return it for processing.

Chapter 4: Conclusion

While there have been many studies that investigate patient doses from fluoroscopy there are few which specifically address occupational doses, most focusing on patient doses, specific cardiac procedures, or general radiation protection. When Kim et al [15] attempted to provide estimated occupational exposures for different interventional procedure types using published clinical data, they were able to find only seven procedures which had at least five sources with published occupational dose data. Even among those seven procedure types, there was a wide variation in the estimated procedural doses because of differences in unit models or the clinical practices in use at different institutions, an issue which was investigated by Hill et al [13]. With the wide variety of interventional procedures, patient demographic groups, and manufacturer/models of interventional systems, it is difficult to find a “one size fits all” approach to optimizing operator dose.

IR operators receive regular radiation safety training and are familiar with basic concepts of dose reduction related to their normal duties, but with their potential for high occupational dose it is imperative that radiation protection and dose reduction remains an integral focus among IR staff. Project 1 of this thesis aimed to contextualize the doses received by IR operators from the units in use at Duke University Hospital.

This information can be used to add specificity to current local training information and emphasize the importance of consistently employing current dose reduction methods. The operators will also be able to better gauge dose effects to themselves of various clinical selections.

This experiment focused on the dose related to changing aspects of patient setup, geometry, and fluoroscopy settings with one x-ray tube positioned directly below the patient table. Similar investigation can be done into the differing aspects of cine as well as possible angular variations or comparisons between the tubes of biplane units. Another possible avenue of investigation is to verify whether Monte Carlo simulations can reproduce these results, as an accurate Monte Carlo simulation could help with developing methods for estimating operator dose without requiring dosimetry data.

Project 2 aimed to address the implementation aspect of dose optimization methods by developing a framework for using historical procedure data to identify areas where dose optimization can be improved upon. The RDSR was initially implemented to capture procedure information related to patient dose, and its application to identifying operator dose trends is a novel approach. The data for most of this analysis was limited to a three-year period and all analysis involving AKRs is limited to data from Year 3 as this was the only dataset which separated the fluoroscopy air kerma contribution from the total air kerma. This framework provides an initial

means of utilizing RDSR data to compare performance of interventional procedures, which can guide dose reduction efforts among IR staff by identifying individuals or areas where improvement of techniques can result in reduction in operator doses.

This framework can be further expanded in multiple ways. The analysis of specific procedures is done on the assumption of a certain level of clinical similarity between types of procedures. Many of the procedure types were unable to be analyzed due to the small number performed over the analysis period, so a deeper study of these could be done if a larger historical dataset were obtained. Additionally, this framework focuses on whole-body occupational doses and does not take into consideration extremity dose to the hands. One of the findings in Kim et al [15] was that operator doses to the hands in biliary tube procedures were much higher than doses to the body. At organizations where IR operators regularly wear extremity dosimeters, it may be beneficial to investigate whether this framework can be modified to include ways to identify trends in extremity dose as well as whole-body dose.

This framework also mainly addresses procedure characteristics related to fluoroscopy and ignores the contribution from cine. As noted in Chapter 2, cine exposure rates to operators are significantly higher than for fluoroscopy. Many procedures which require cine also have longer imaging times and therefore these procedures contribute more significantly to operator dose than the four procedure

categories analyzed in this study. A more detailed characterization of the effects of continuous cine and spot images could help derive analysis methods that address these differences and mitigating them could lead to a more substantial reduction in operator dose.

This thesis is meant to be a tool for hospital radiation safety staff to aid in assessing the radiation safety performance of their IR operators, specifically if individuals in question are routinely at risk of exceeding their occupational dose limits. The methods in Project 1 will provide site-specific information about the variations between IR systems being used clinically and the effects on operator occupational exposure from local protection measures. The framework outlined in Project 2 can then be used to analyze variations in completed procedures that impact operator doses. Once an initial assessment is done, radiation safety staff can work with IR departmental leadership to develop customized training procedures or adjustments of current clinical techniques to optimize operator doses.

References

- [1] Miller, D. L. (2008). Overview of contemporary interventional fluoroscopy procedures. *Health Physics*, 95(5), 638–644. <https://doi.org/10.1097/01.HP.0000326341.86359.0B>
- [2] Taslakian, B., Ingber, R., Aaltonen, E., Horn, J., & Hickey, R. (2019). Interventional Radiology Suite: A Primer for Trainees. *Journal of Clinical Medicine*, 8(9). <https://doi.org/10.3390/JCM8091347>
- [3] *X-ray Production, Tubes, and Generators* | *Radiology Key*. (n.d.). Retrieved February 12, 2023, from <https://radiologykey.com/x-ray-production-tubes-and-generators/#F1-6>
- [4] Bushberg, J. T. (2012). *The essential physics of medical imaging*. Wolters Kluwer Health/Lippincott Williams & Wilkins.
- [5] *Allura Xper FD20* | *Philips*. (n.d.). Retrieved February 12, 2023, from <https://www.philips.co.in/healthcare/product/HC722012CA/allura-xper-fd20-cardiovascular-x-ray-system>
- [5] NRC: 10 CFR 20.1201 Occupational dose limits for adults. (n.d.). Retrieved February 13, 2023, from NRC: <https://www.nrc.gov/reading-rm/doc-collections/cfr/part020/part020-1201.html>
- [7] Garg, T., & Shrigiriwar, A. (2021). Radiation Protection in Interventional Radiology. *The Indian Journal of Radiology & Imaging*, 31(4), 939. <https://doi.org/10.1055/S-0041-1741049>
- [8] Kim JH. Three principles for radiation safety: time, distance, and shielding. *Korean J Pain*. 2018 Jul;31(3):145-146. doi: 10.3344/kjp.2018.31.3.145. Epub 2018 Jul 2. PMID: 30013728; PMCID: PMC6037814.
- [9] Philips Healthcare (2014) *ClarityIQ technology* [White paper]. <https://www.philips.com.co/c-dam/b2bhc/co/landing/azurion/whitepaper-clarity-iq.PDF>.
- [10] Vanzant, D., & Mukhdomi, J. (2022). Safety of Fluoroscopy in Patient, Operator, and Technician. *StatPearls*. <https://www.ncbi.nlm.nih.gov/books/NBK570567/>

- [11] *ATOM® Phantom Family - CIRS*. (n.d.). Retrieved February 12, 2023, from <https://www.cirsinc.com/products/radiation-therapy/atom-phantom-family/>
- [12] *Measuring Radiation | NRC.gov*. (n.d.). Retrieved March 2, 2023, from <https://www.nrc.gov/about-nrc/radiation/health-effects/measuring-radiation.html>
- [13] Hill KD, Mann SD, Carboni MP, Doyle TP, Idriss SF, Janssen DF, Nicholson GT, Sathanandam S, Fleming GA. Variability in radiation dose and image quality: A comparison across fluoroscopy-system vendors, generations of equipment and institutions. *Catheter Cardiovasc Interv*. 2018 Dec 1;92(7):E471-E477. doi: 10.1002/ccd.27793. Epub 2018 Sep 12. PMID: 30208245; PMCID: PMC6294676.
- [14] Understanding and Choosing the Right Probability Distributions. (2012). In *Advanced Analytical Models* (pp. 899–917). <https://doi.org/10.1002/9781119197096.app03>
- [15] Kim KP, Miller DL, Berrington de Gonzalez A, Balter S, Kleinerman RA, Ostroumova E, Simon SL, Linet MS. Occupational radiation doses to operators performing fluoroscopically-guided procedures. *Health Phys*. 2012 Jul;103(1):80-99. doi: 10.1097/HP.0b013e31824dae76. PMID: 22647920; PMCID: PMC3951010.